Metallic films: conductivity properties vs. work function. New opportunities for accelerators and other technological applications

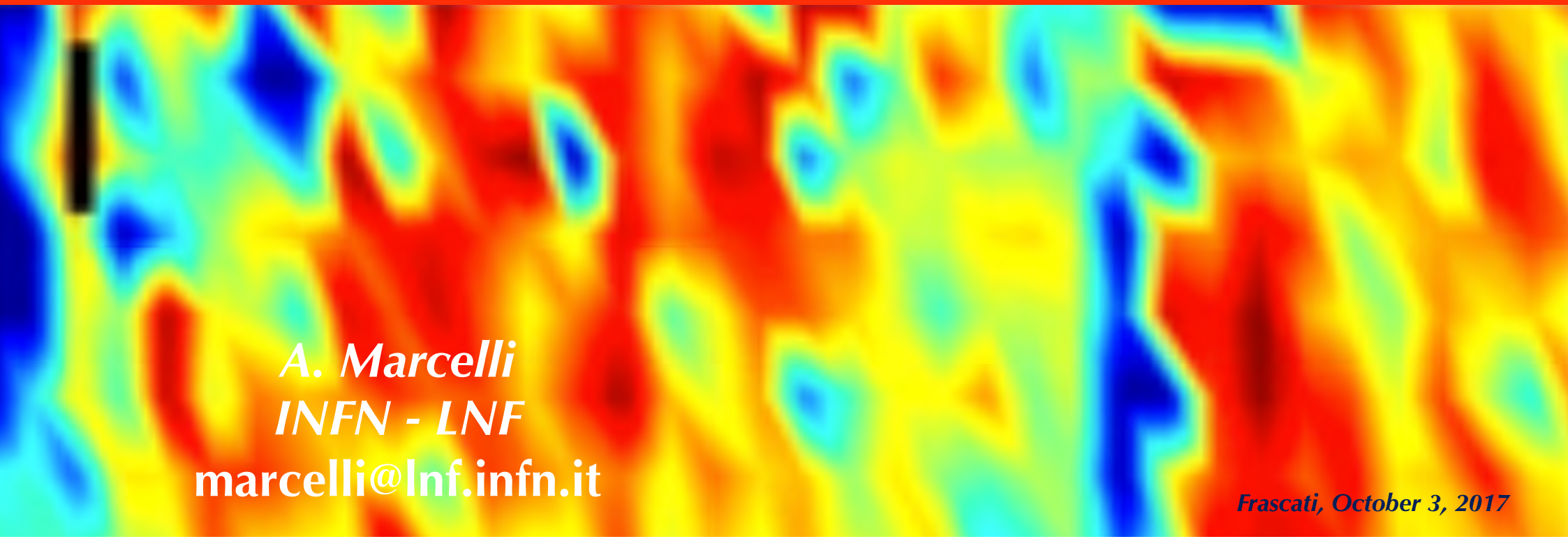

A. Marcelli
INFN - LNF
marcelli@lnf.infn.it

Frascati, October 3, 2017

Layout

- Introduction: materials, breakdown rates, work function, etc.
- Mesoscale science, metals, alloys and TM oxides
- The case of Mo and MoO_3 coatings
- Perspectives & conclusions

Frascati, October 3, 2017

Accelerating field limits

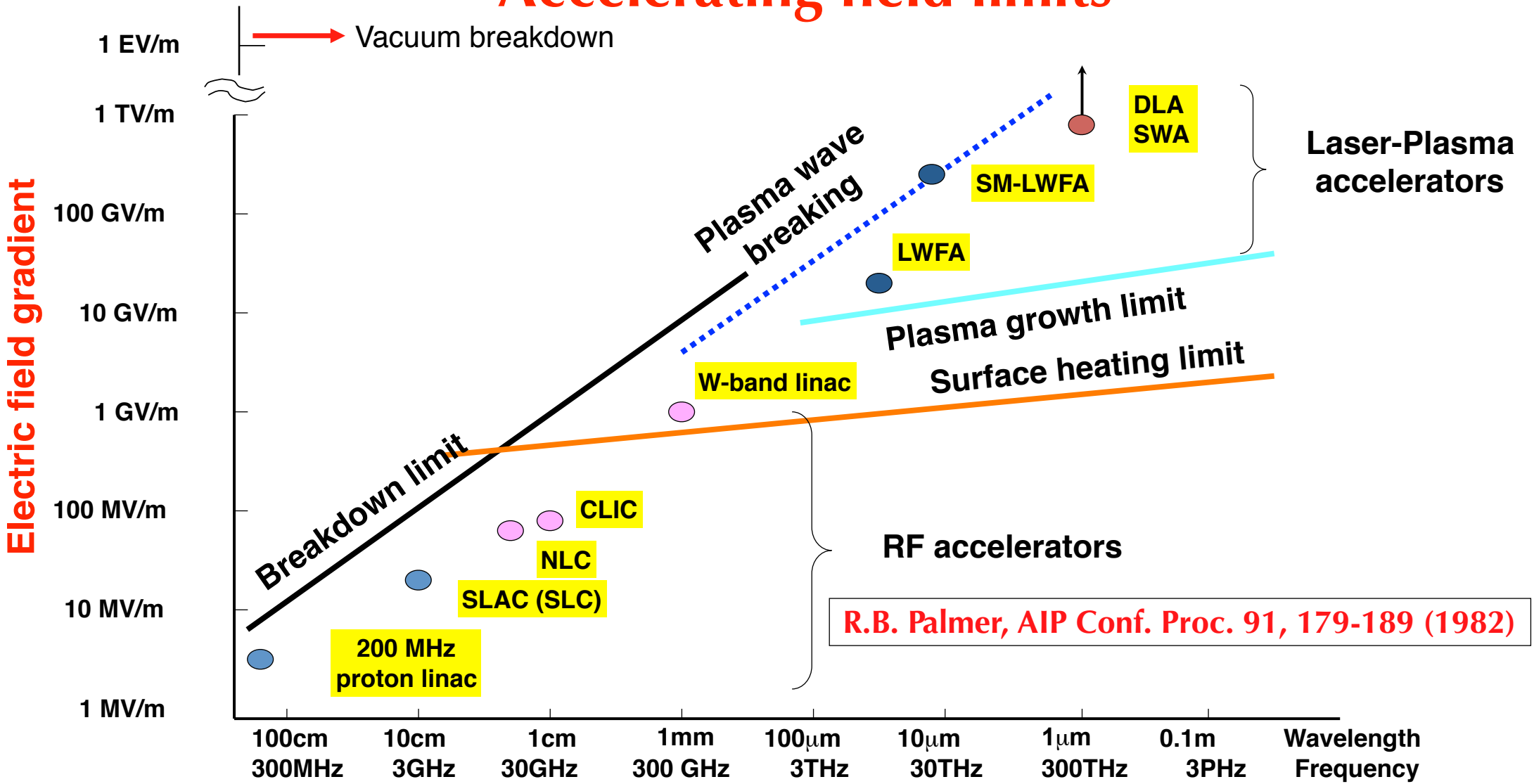

R.B. Palmer, AIP Conf. Proc. 91, 179-189 (1982)

Exponential growth

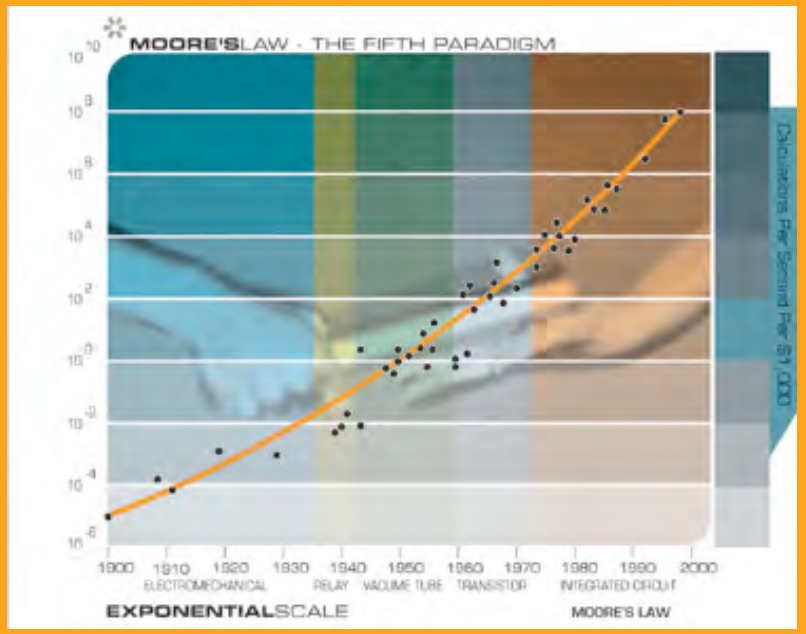

Moore law

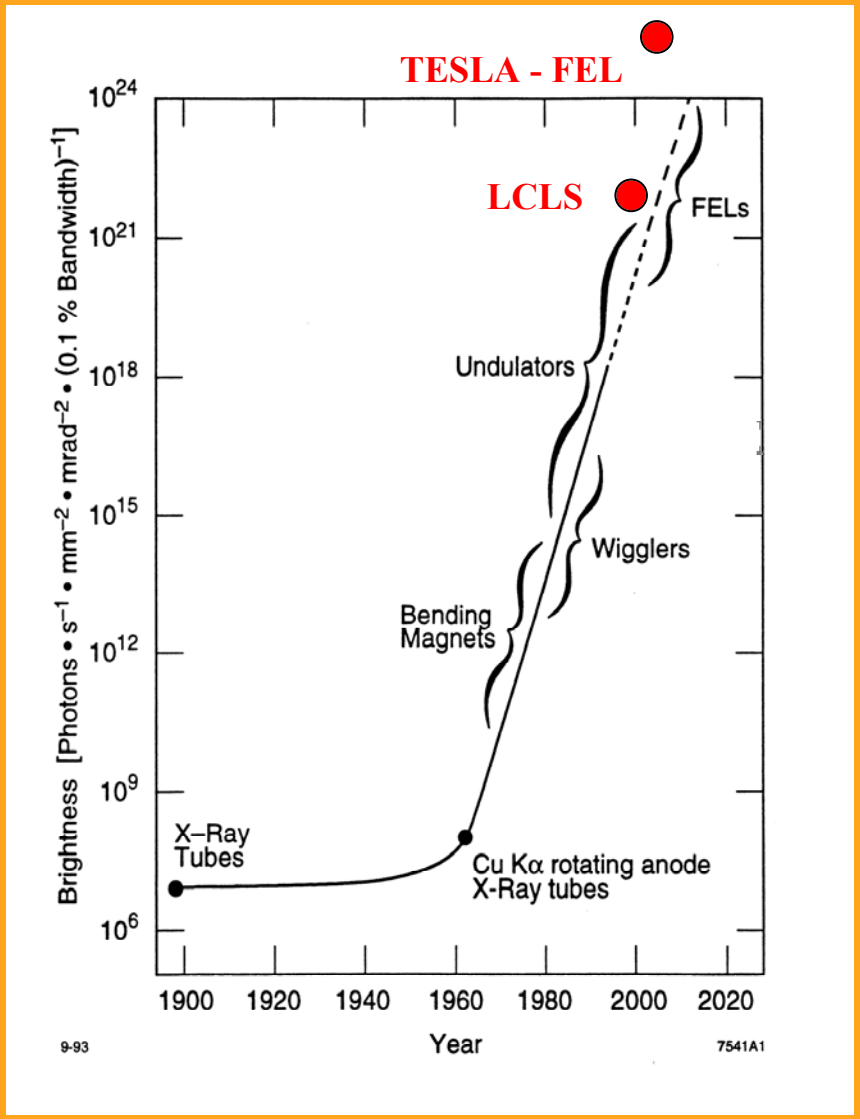

Frascati, October 3, 2017

Comparison of peak pulse heating for two Cu and one Mo structure [*shaped* pulse, flat part 150 ns]

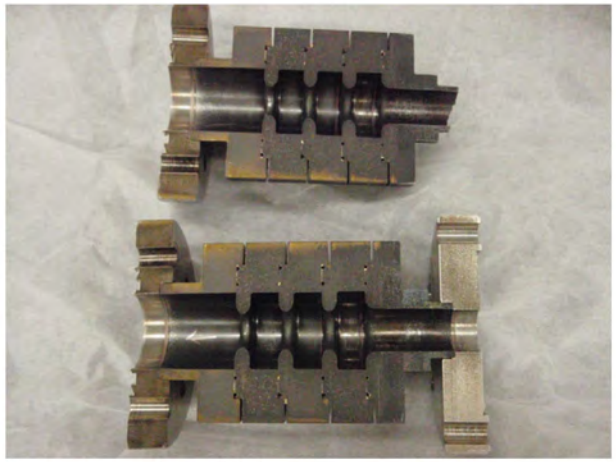

Spataro et al. NIM-A-657 (2011) 114-121

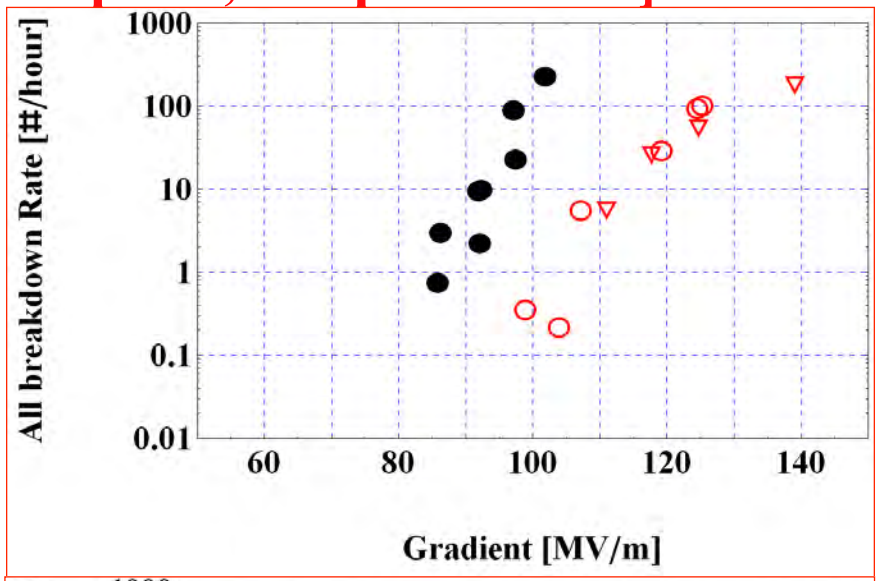

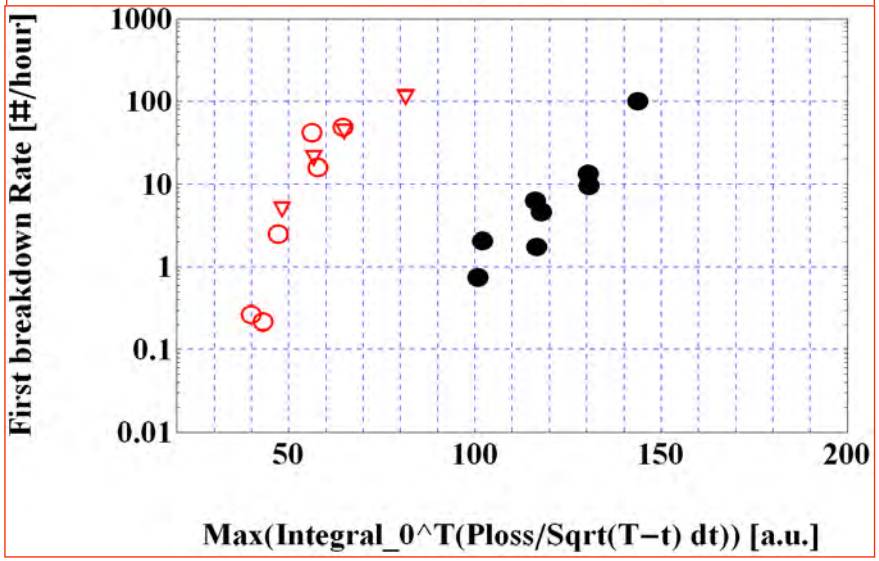

Frascati, October 3, 2017

On the materials basis of modern society

T. E. Graedel[1], E. M. Harper, N. T. Nassar, and Barbara K. Reck

School of Forestry and Environmental Studies, Center for Industrial Ecology, Yale University, New Haven, CT 06511

Edited by William C. Clark, Harvard University, Cambridge, MA, and approved October 11, 2013 (received for review July 29, 2013)

www.pnas.org/cgi/doi/10.1073/pnas.1312752110

Significance

Modern life is enabled by the use of materials in its technologies. Over time, these technologies have used a larger and more diverse array of materials. Elemental life cycle analyses yield an understanding of these materials, and a definite concern that arises is that of possible scarcity of some of the elements as their use increases. We studied substitution potential for 62 different metals in their major uses. For a dozen different metals, the potential substitutes for their major uses are either inadequate or appear not to exist at all. Further, for not 1 of the 62 metals are exemplary substitutes available for all major uses.

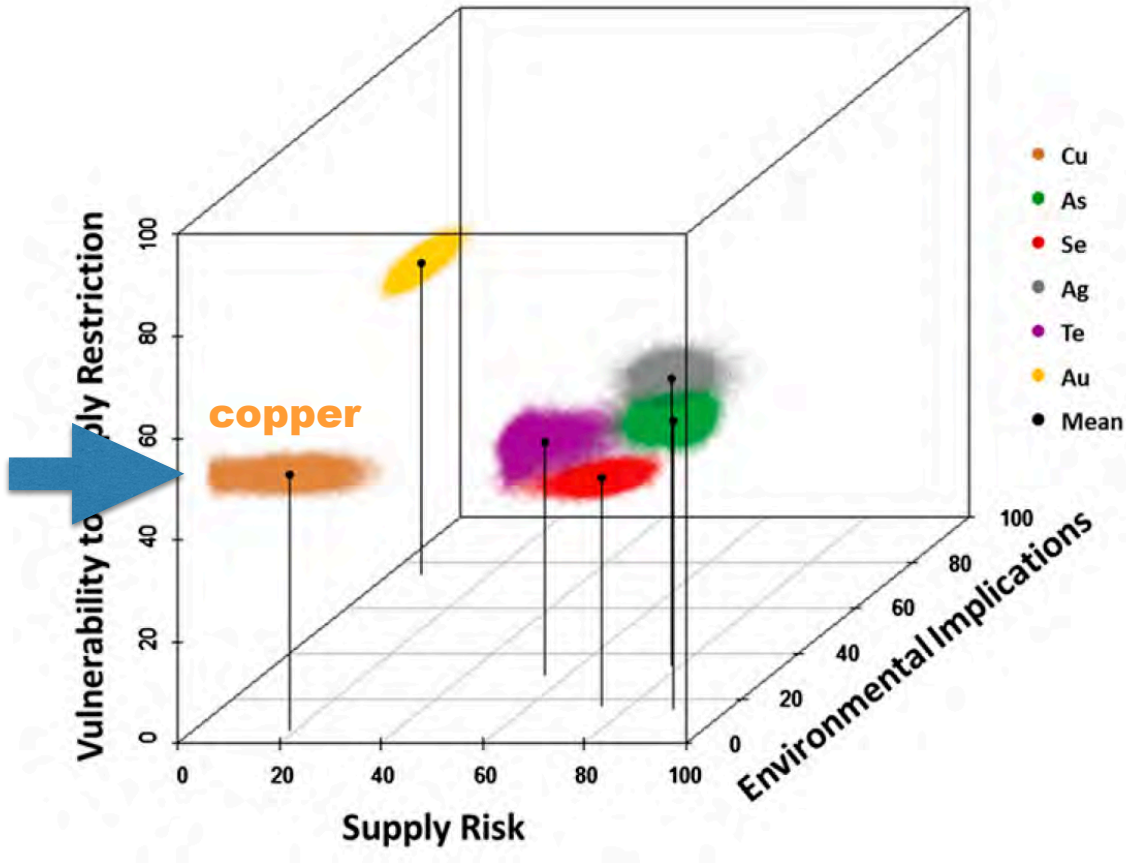

PRL 115, 264802 (2015) PHYSICAL REVIEW LETTERS week ending 31 DECEMBER 2015

Observation of Field-Emission Dependence on Stored Energy

Jiahang Shao,[1,2,*] Sergey P. Antipov,[2,3] Sergey V. Baryshev,[2,3] Huaibi Chen,[1] Manoel Conde,[2] Darrell S. Doran,[2] Wei Gai,[2] Chunguang Jing,[2,3] Wanming Liu,[2] John Power,[2] Jiaqi Qiu,[2,3] Jiaru Shi,[1] Dan Wang,[1,2] Faya Wang,[4,†] Charles E. Whiteford,[2] Eric Wisniewski,[2] and Liling Xiao[4]

[1]*Department of Engineering Physics, Tsinghua University, Beijing 100084, People's Republic of China*
[2]*Argonne National Laboratory, Lemont, Illinois 60439, USA*
[3]*Euclid Techlabs LLC, Solon, Ohio 44139, USA*
[4]*SLAC National Accelerator Laboratory, Menlo Park, California 94025, USA*

(Received 24 August 2015; published 23 December 2015)

Field emission from a solid metal surface has been continuously studied for a century over macroscopic to atomic scales. It is general knowledge that, other than the surface properties, the emitted current is governed solely by the applied electric field. A pin cathode has been used to study the dependence of field emission on stored energy in an *L*-band rf gun. The stored energy was changed by adjusting the axial position (distance between the cathode base and the gun back surface) of the cathode while the applied electric field on the cathode tip is kept constant. A very strong correlation of the field-emission current with the stored energy has been observed. While eliminating all possible interfering sources, an enhancement of the current by a factor of 5 was obtained as the stored energy was increased by a factor of 3. It implies that under certain circumstances a localized field emission may be significantly altered by the global parameters in a system.

DOI: 10.1103/PhysRevLett.115.264802 PACS numbers: 29.20.Ej, 52.80.Pi, 79.70.+q

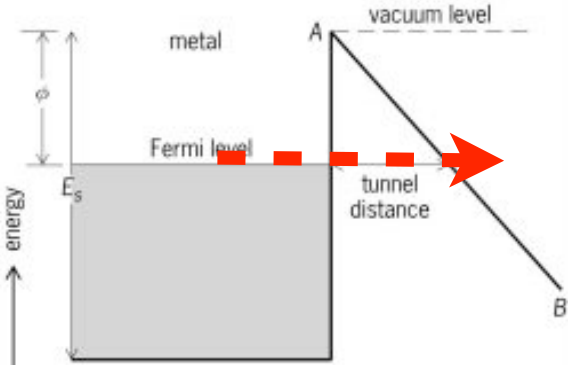

Istituto Nazionale di Fisica Nucleare

Two well-known special barrier forms exist:

Exact triangular (ET) barrier

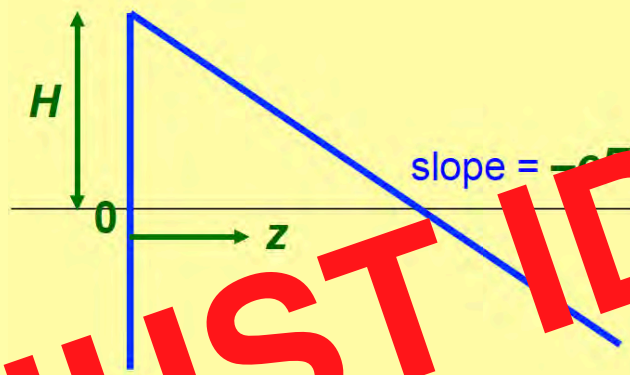

$M(z) = H - eFz$

used by **Fowler & Nordheim**

Schottky-Nordheim (SN) barrier

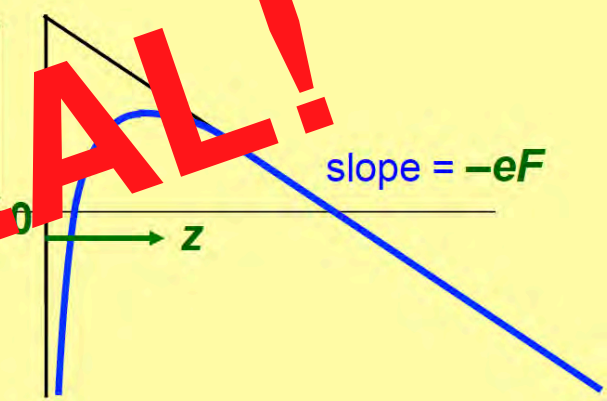

$M(z) = H - eFz - 1/16\pi\varepsilon_0 z$

used by **Murphy & Good**

JUST IDEAL!

Frascati, October 3, 2017

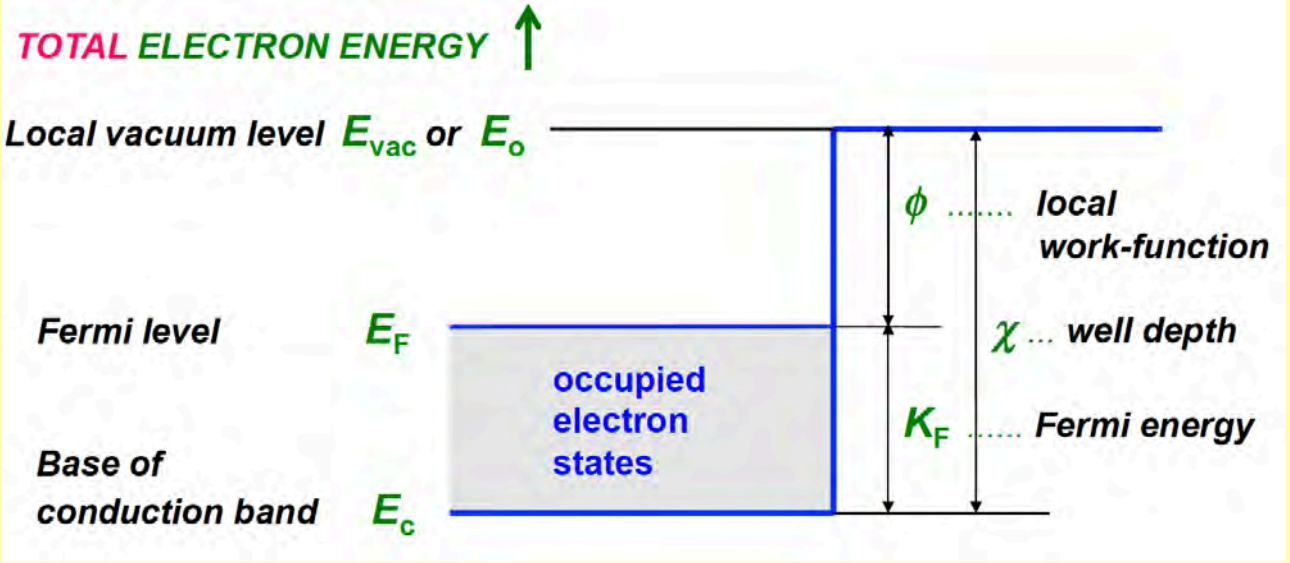

The well depth and the local work-function have TWO components

- **a bulk (or "chemical") component**
- **a surface (or "electric dipole") component.**

The bulk component explains why different materials have different work functions; the surface component explains why different faces of a single material have different work-functions.

In summary, a strong correlation between the field-emission current and the stored energy has been observed on pin cathodes. This study has excluded mechanisms that may affect the conclusion, such as multipacting in the cavity, background emission from other surfaces, secondary electron emission from the Faraday cup, the beam loading effect, and the space charge limited emission effect. We conclude that the observation is fundamental and inconsistent with the Fowler-Nordheim equation. This indicates that macroscopic parameters like stored energy are affecting the microscopic emission. The findings suggest a new territory to be explored while developing field emission electron sources and high gradient devices.

Jahang Shao et al. Phys Rev. Lett. 115, 264802 (2015)

Autopsy of an electroformed Au-Ni structure

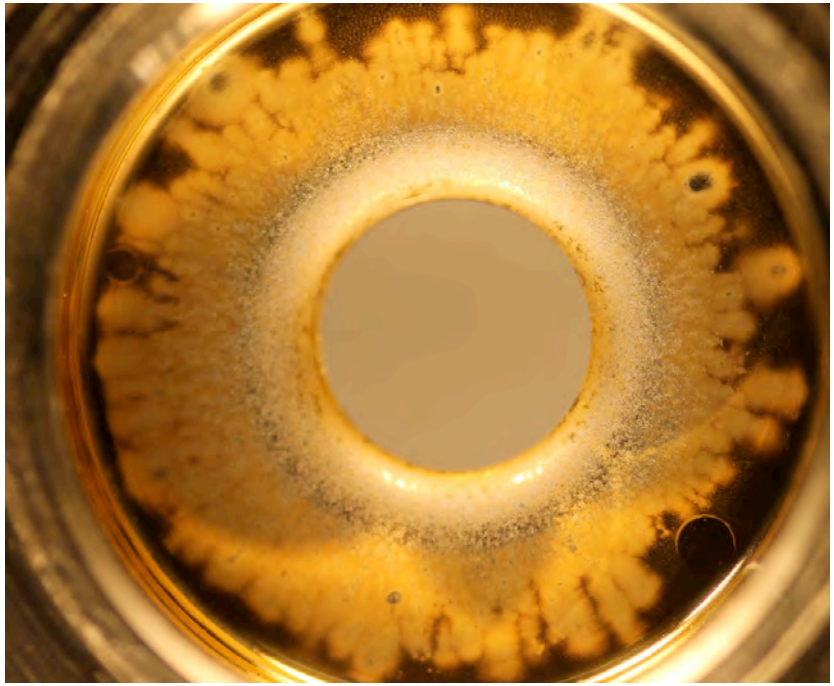

High gradient side of
Center cell

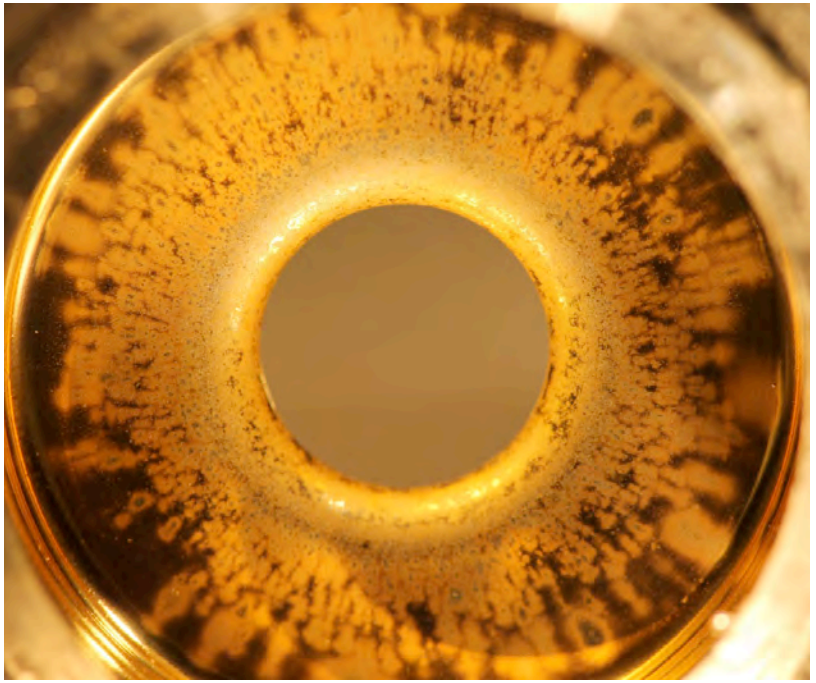

High gradient side of
End cell

Au coating is removed from the high-electric field area by multiple breakdowns

Courtesy V. Dolgashev (SLAC)

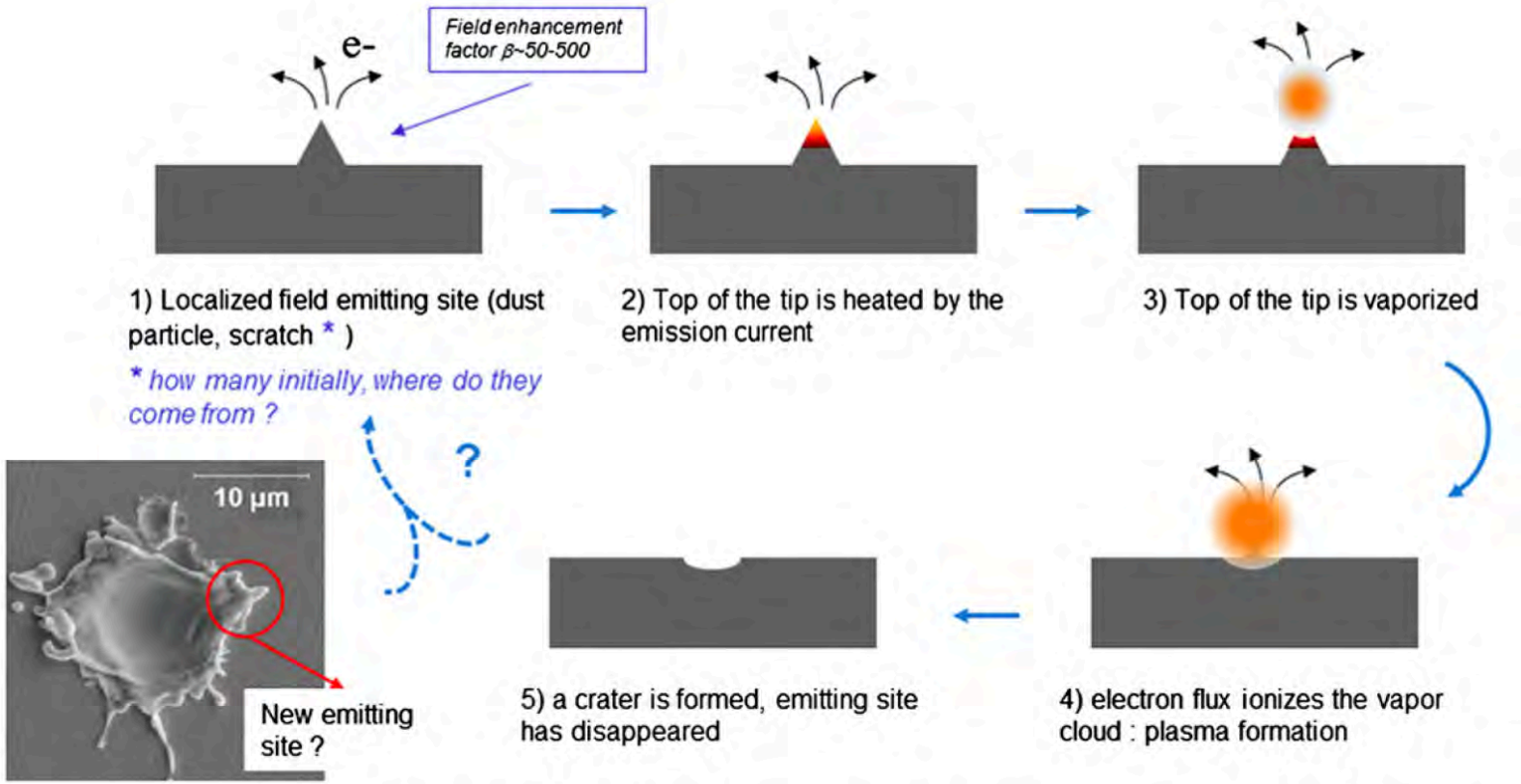

Fig. 3. Classical breakdown scenario: BD is initiated by a local defect (inclusions, dust particle, cutting flake, etc.) which provide sufficient field enhancement to induce field emission. The current at the apex of the emitting site becomes sufficient to heat up and vaporize the material, where the emitting current can trigger plasma and generate the explosion of the emitting site. This scenario does not consider the origin of emitting sites.

Antoine et al, Nuclear Instruments and Methods in Physics Research A 665 (2011) 54–69

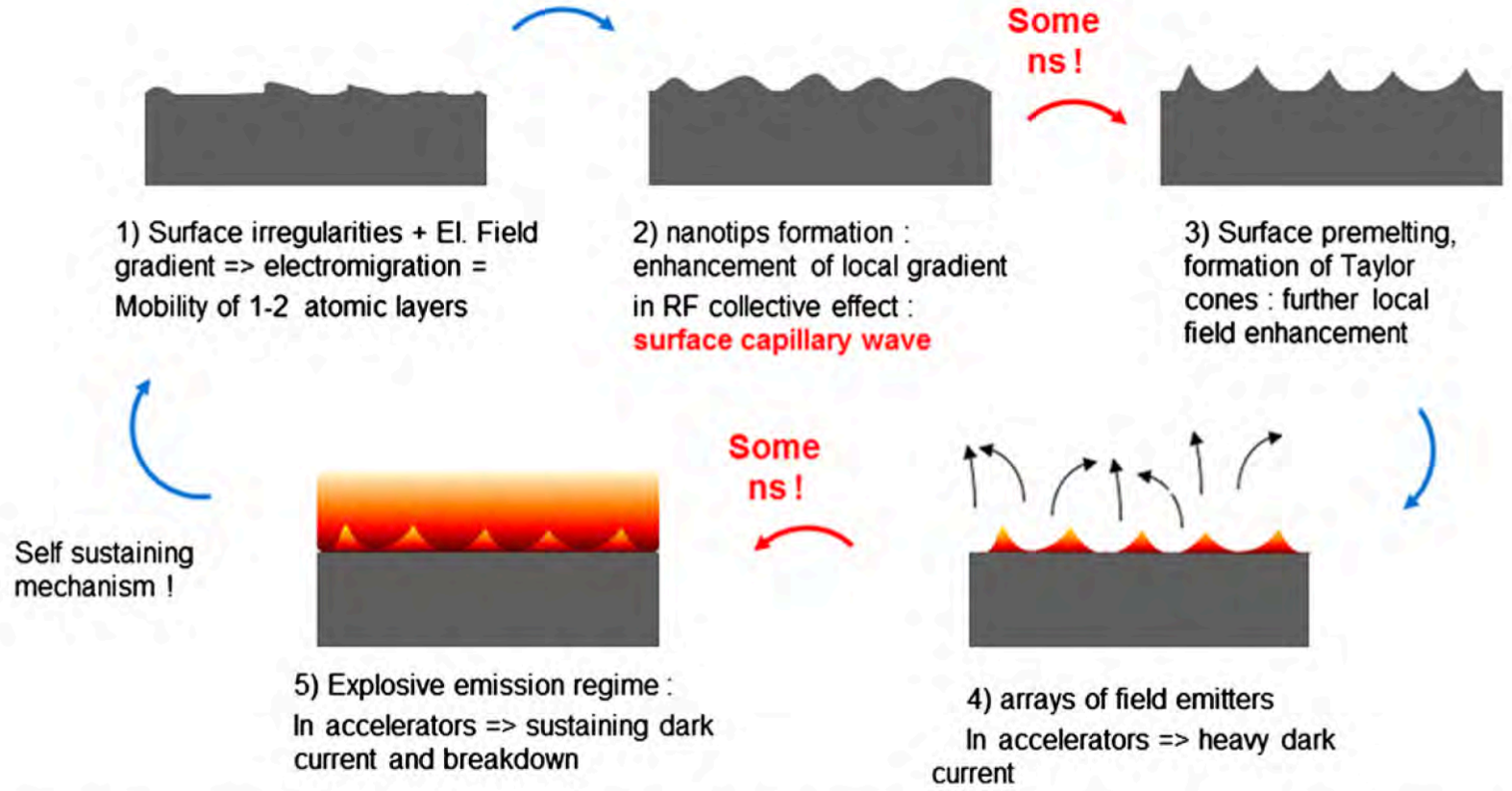

Fig. 4. Alternative scenario for breakdown: electromigration tends to enhance the surface irregularities because atoms tend to migrate along field gradient toward the top of the "hill" and form nanotips. In certain conditions, such as the presence of RF field, this effect becomes collective and will help form an array of nanotips. Once this phenomena starts, it can only run away because the electric field gradient become stronger, which in turn enhances electromigration, etc. until the surface becomes liquid like. The electromigration scenario shows that in some conditions, emitters can be formed simply due to the presence of electric field and can trigger breakdown continuously (see text for details).

Autopsy of an electroformed Au-Ni structure

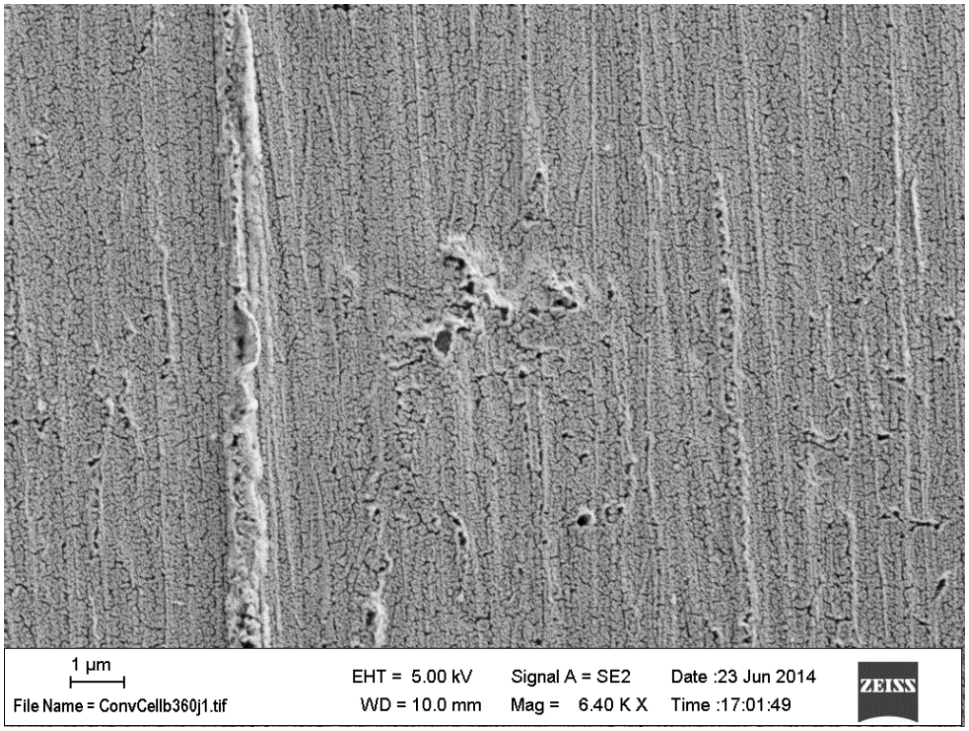

Coupler cell, near 2b diameter, low pulse heating area

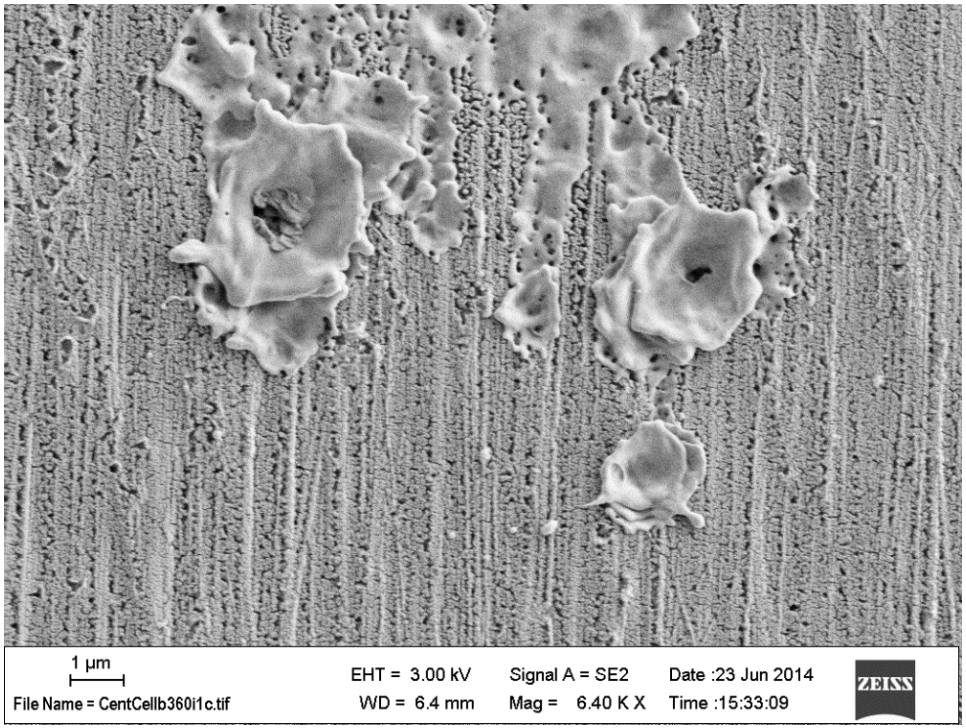

Center cell, high pulse heating area

Courtesy V. Dolgashev (SLAC)

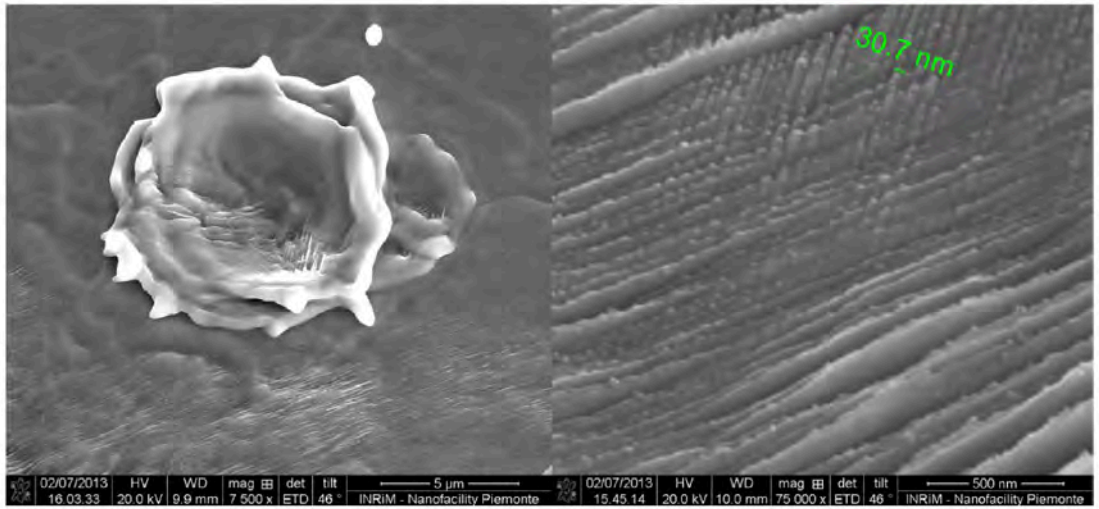

Fig. 4. Details of the surface of a cavity exposed at SLAC (courtesy of V. Dolgashev). left) an isolated defect consisting in a molten Cu crater showing the texture ascribed to thermal fatigue; right) a magnified view of texture at the nanometer scale induced by the cyclic pulsed heating.

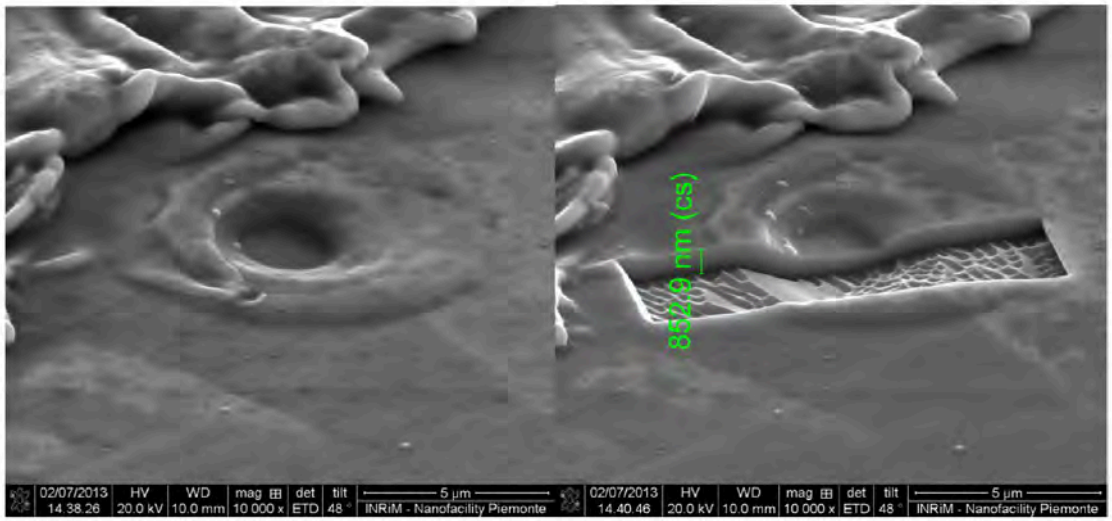

Fig. 5. Left: damaged copper surface at the boundary of fully melted regions near the iris of a cell (cavity exposed at SLAC-courtesy of V. Dolgashev). Right: the typical depth of the isolated corona damage is of the order of few micrometers as shown by the FIB cross section.

Courtesy V. Dolgashev (SLAC)

Next Generation High Brightness Electron Beams From Ultra-High Field Cryogenic Radiofrequency Photocathode Sources

J.B. Rosenzweig[1], A. Cahill[1], V. Dolgashev[2], C. Emma[1], A. Fukusawa[1], R. Li[2], C. Limborg[2], J. Maxson[1], P. Musumeci[1], A. Nause[1], R. Pakter[1], R. Pompili[3], R. Roussel[1], B. Spataro[3], and S. Tantawi[2]

[1]*Department of Physics and Astronomy, University of California, Los Angeles*

[2]*Stanford Linear Accelerator Laboratory, Stanford University*

[3]*Istituto Nazionale di Fisica Nucleare, Laboratori Nazionali di Frascati, Frascati, Italy*

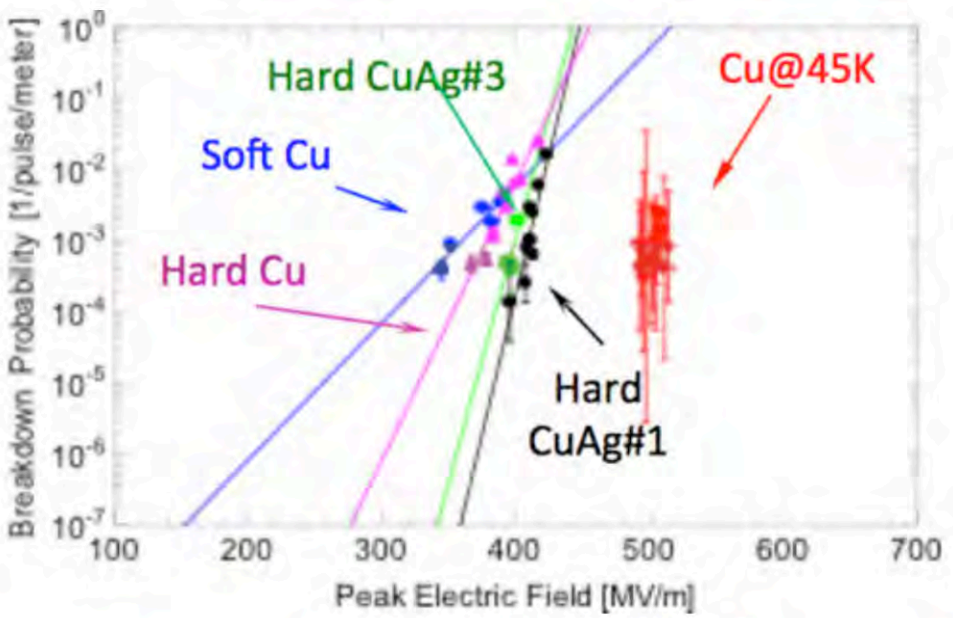

Figure 2. Breakdown probability as a function of peak electric field in single cell X-band accelerating structure tests. The introduction of a harder alloy improves the breakdown as predicted; the effect of operation at 45 deg K is more dramatic, permitting surface electric fields of 500 MV/m.

INFN
Istituto Nazionale di Fisica Nucleare

TABLE II. Fundamental constants for copper.

Thermal conductivity [W/m K]	400
Volumetric heat capacity [MJ/m^3 K]	3.45
Resistivity@300 K [nΩ m]	17
Melting temperature [K]	1358

The advantages conferred by cryogenic operation of RF cavities for high field operation arise from the hardness of the material, the lowered surface dissipation and concomitant pulsed heating.

The improved yield strength of the copper material (new alloys?) is the effect that enables very high fields to be reached, while the changes in dissipation dictate important design features of the RF cavity system in its practical manifestation.

Frascati, October 3, 2017

INFN
Istituto Nazionale di Fisica Nucleare

Mesoscale science

Mesoscale science, where atomic granularity, quantization of energy, and simplicity of structure and function give way to continuous matter and energy, complex structures, and composite functionalities, is a broad and rich horizon for innovative materials and chemistry.

We assisted to a continuous increase of investigations at ever smaller length and time scales that reveal the atomic, molecular, and nanoscale origins of macroscopic behaviour. Now, we have to begun to reverse the approach, using the knowledge of nanoscale phenomena to understand and control mesoscale architectures to promote the emergence of new behaviours.

Actually the mesoscale is an inherently dynamic regime, where energy and information captured at the nanoscale are processed and transformed at the mesoscale. Experiments have to look at the dynamics, possibly *in situ*, and have to be multimodal being the ordinary "static" characterisation not more sufficient.

Frascati, October 3, 2017

Philosophical Magazine
Vol. 90, No. 11, 14 April 2010, 1451–1464

Mesoscale strain measurement in deformed crystals: A comparison of X-ray microdiffraction with electron backscatter diffraction

D.P. Field[a]*, K.R. Magid[b], I.N. Mastorakos[a], J.N. Florando[c], D.H. Lassila[c] and J.W. Morris Jr.[d]

[a]*School of Mechanical and Materials Engineering, Washington State University, Pullman, WA 99164-2920, USA;* [b]*Laboratory for Nanometallurgy, Department of Materials, ETH-Zurich, CH-8093 Zurich, Switzerland;* [c]*Lawrence Livermore National Laboratory, Livermore, CA 94551, USA;* [d]*Department of Materials Science and Engineering, University of California, Berkeley, CA 94720, USA*

(*Received 29 June 2009; final version received 6 October 2009*)

Frascati, October 3, 2017

Philosophical Magazine
Vol. 90, No. 11, 14 April 2010, 1451–1464

Taylor & Francis
Taylor & Francis Group

Mesoscale strain measurement in deformed crystals: A comparison of X-ray microdiffraction with electron backscatter diffraction

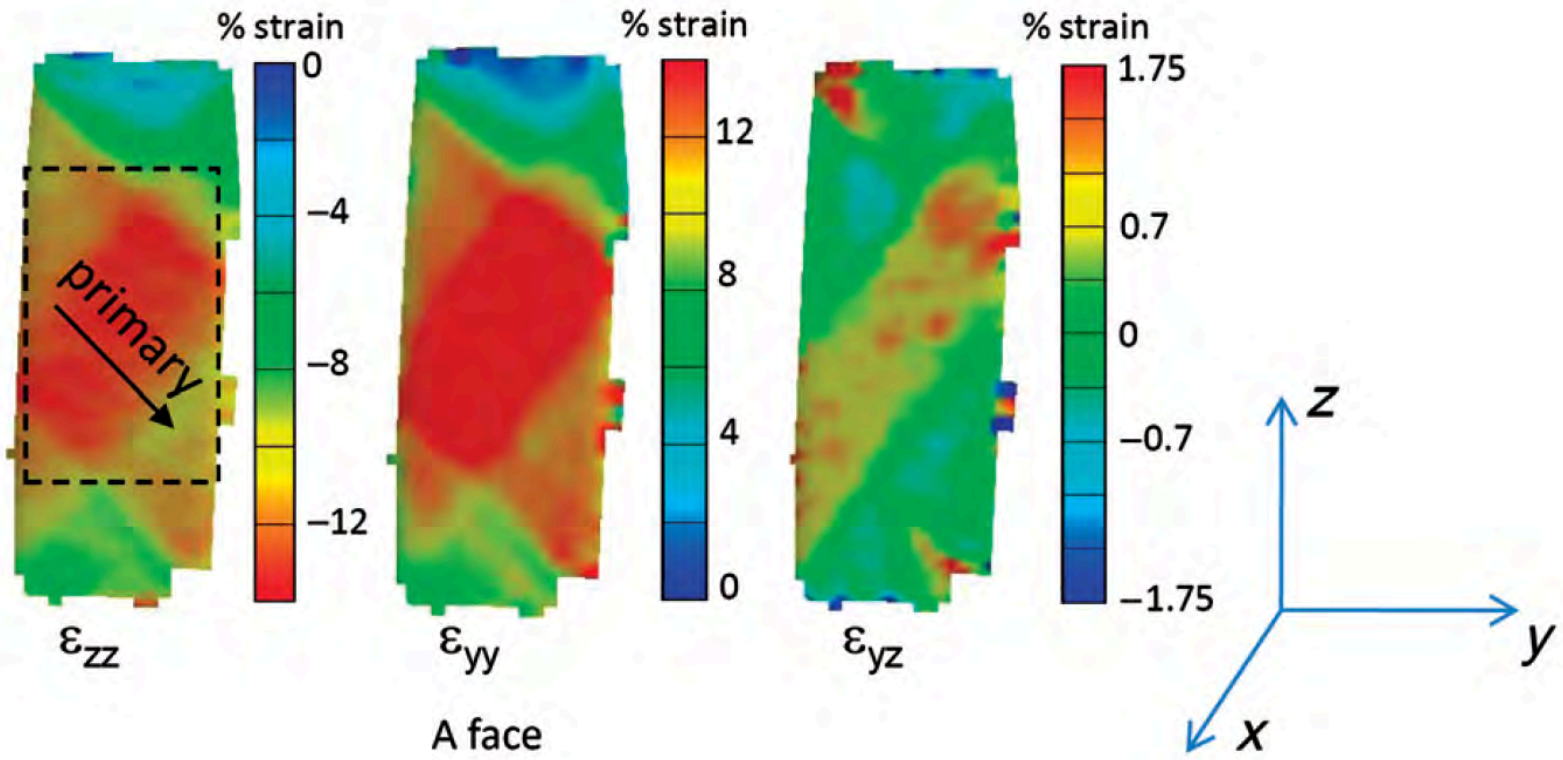

Philosophical Magazine
Vol. 90, No. 11, 14 April 2010, 1451–1464

Taylor & Francis
Taylor & Francis Group

INFN
Istituto Nazionale di Fisica Nucleare

Mesoscale strain measurement in deformed crystals: A comparison of X-ray microdiffraction with electron backscatter diffraction

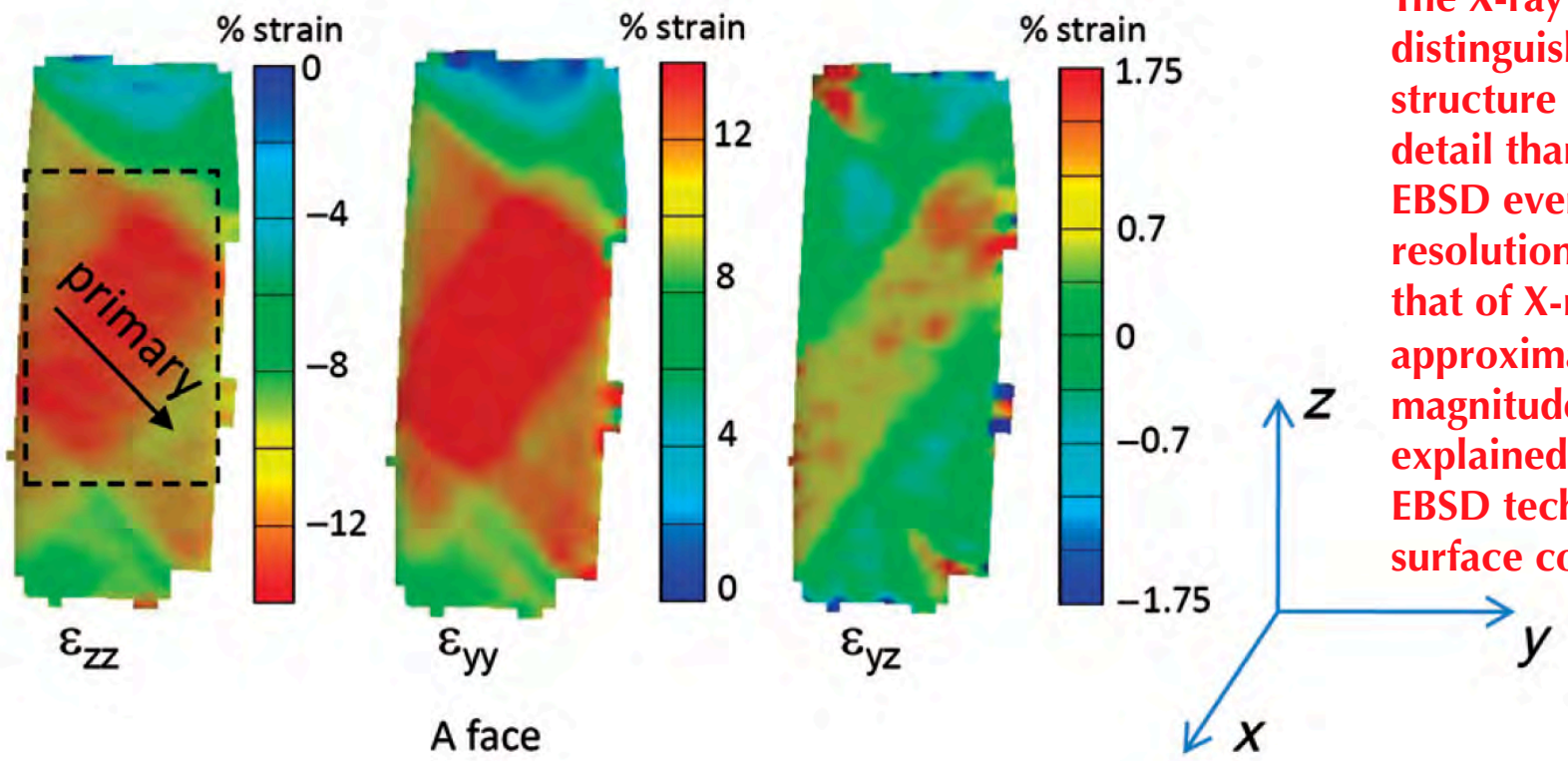

The X-ray technique can distinguish features in the structure that are much finer in detail than those observed using EBSD even though the spatial resolution of EBSD is superior to that of X-ray diffraction by approximately two orders of magnitude. The results are explained by the sensitivity of the EBSD technique to the specimen surface condition.

Philosophical Magazine
Vol. 90, No. 11, 14 April 2010, 1451–1464

Taylor & Francis
Taylor & Francis Group

INFN
Istituto Nazionale di Fisica Nucleare

Mesoscale strain measurement in deformed crystals: A comparison of X-ray microdiffraction with electron backscatter diffraction

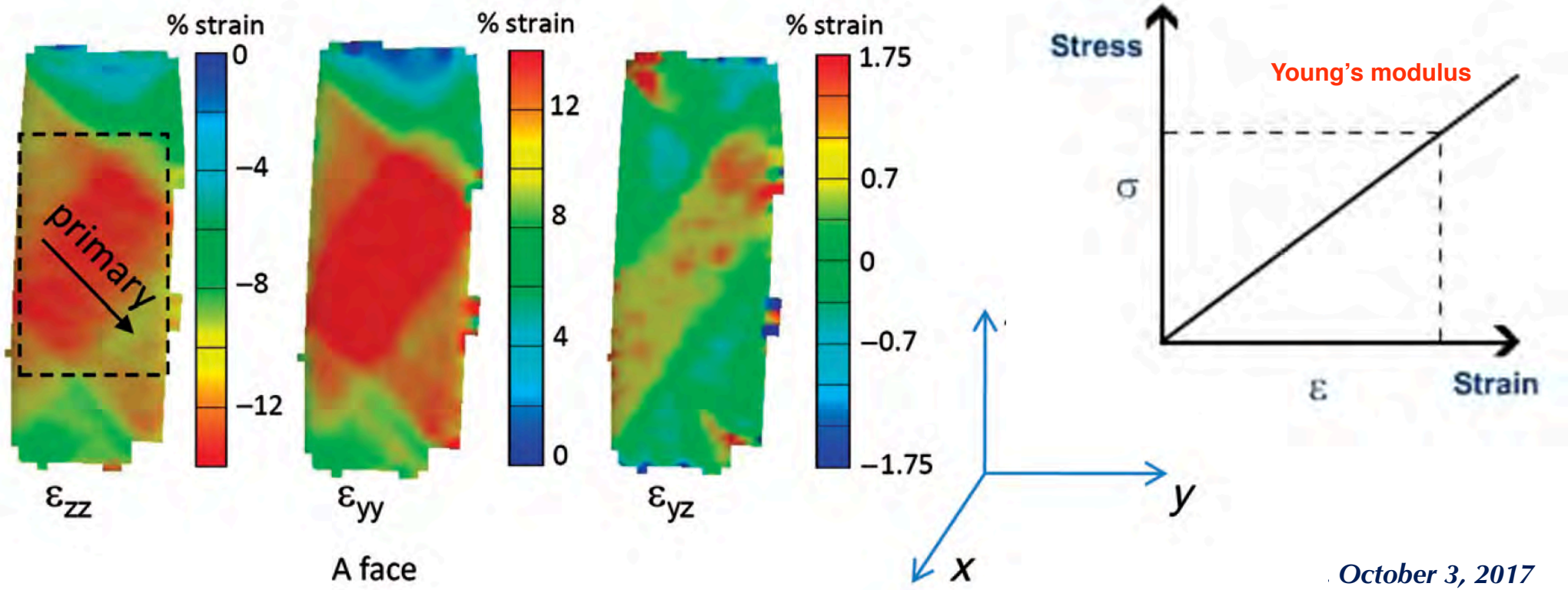

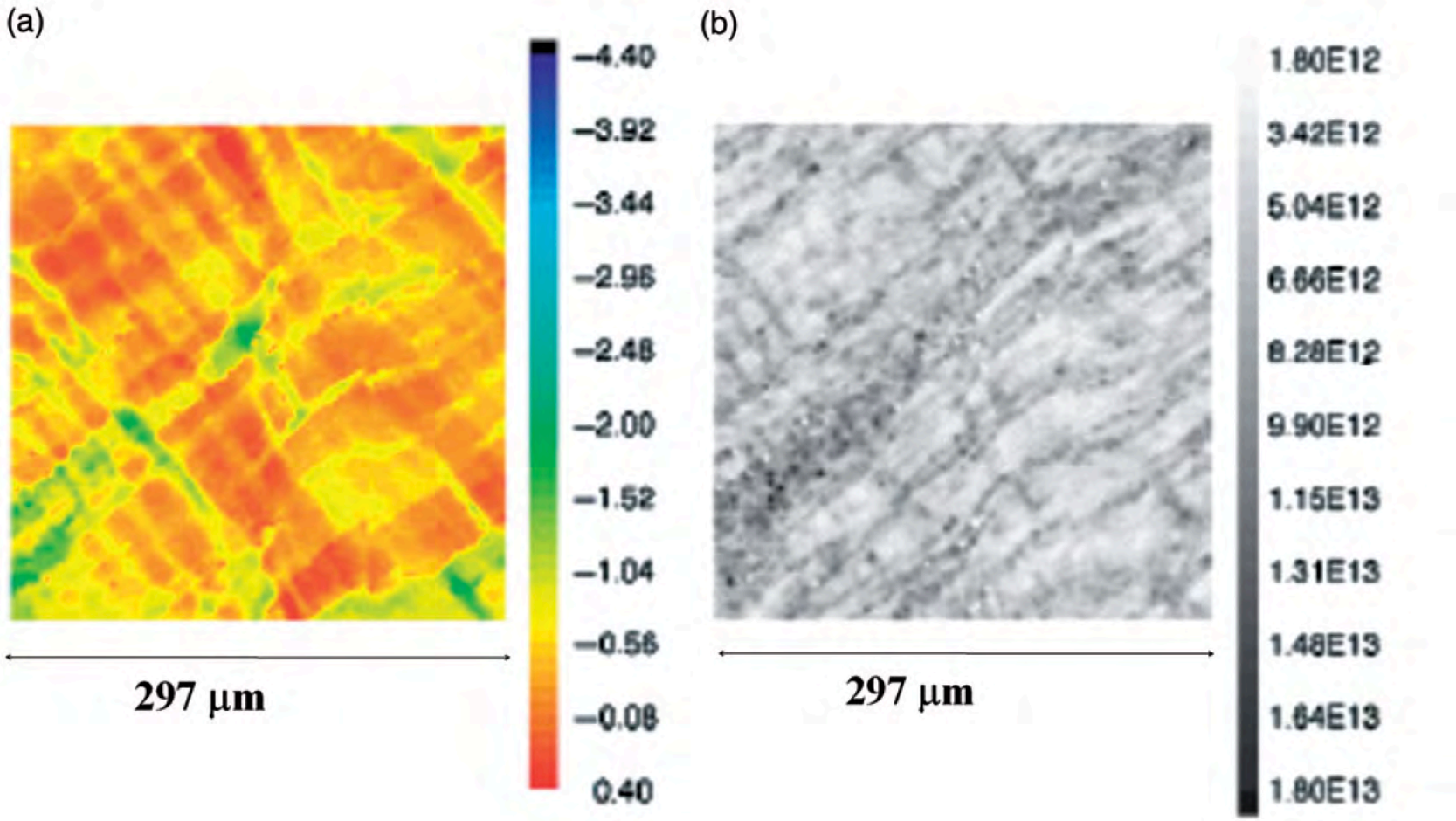

Figure 3. (Colour online). X-ray microdiffraction results showing (a) orientation image and (b) dislocation density map of the deformed structure.

Philosophical Magazine
Vol. 90, No. 11, 14 April 2010, 1451–1464

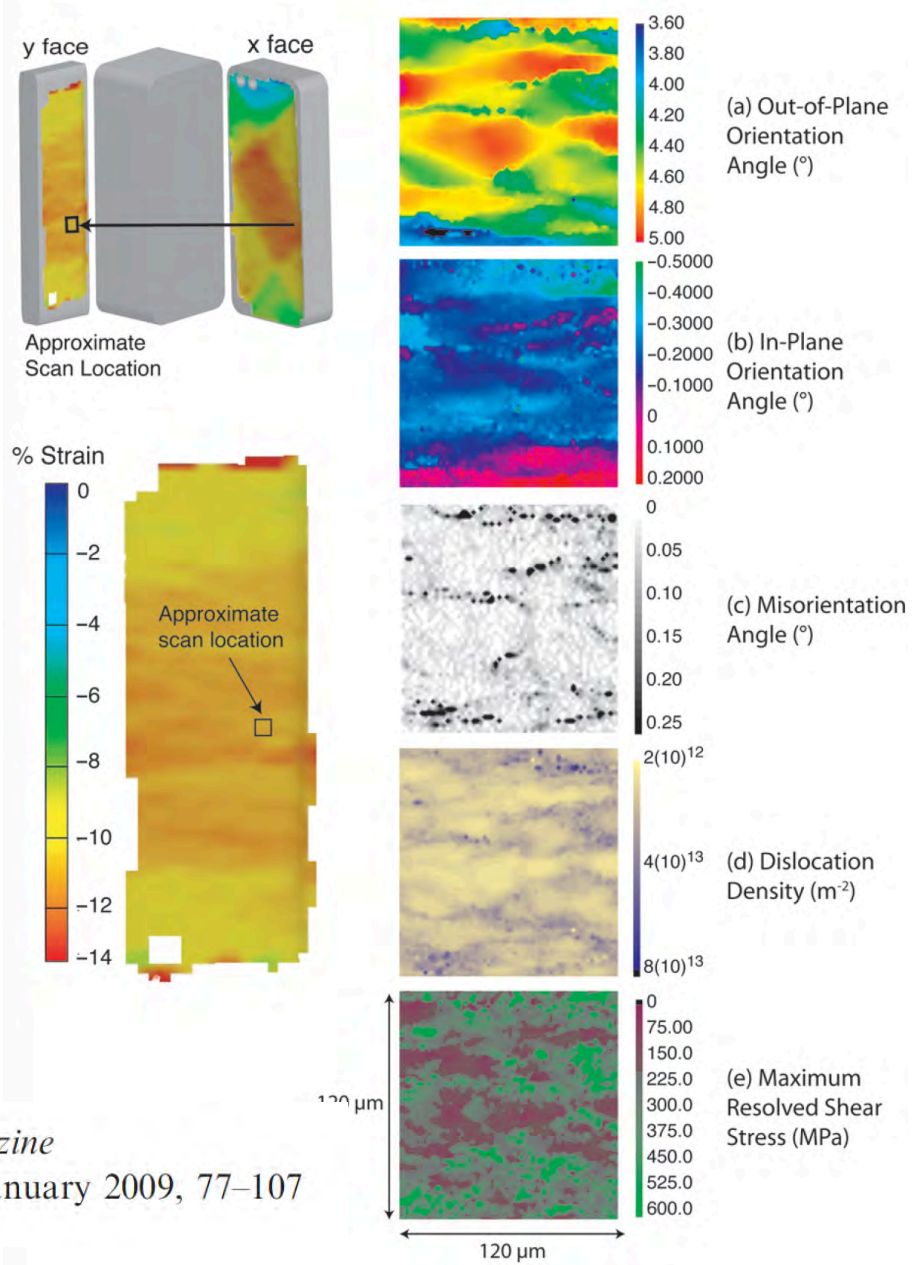

Philosophical Magazine
Vol. 89, No. 1, 1 January 2009, 77–107

It is practical and useful to employ 'multiscale characterization' with modern tools to clarify the nature and interaction of the heterogeneous deformation patterns and mechanisms that operate at different length scales. In particular, the combination of image correlation techniques to map the macroscopic strain and synchrotron (or EBSD) techniques provides detailed information on mesoscopic defect patterns.

Frascati, October 3, 2017

INFN
Istituto Nazionale di Fisica Nucleare

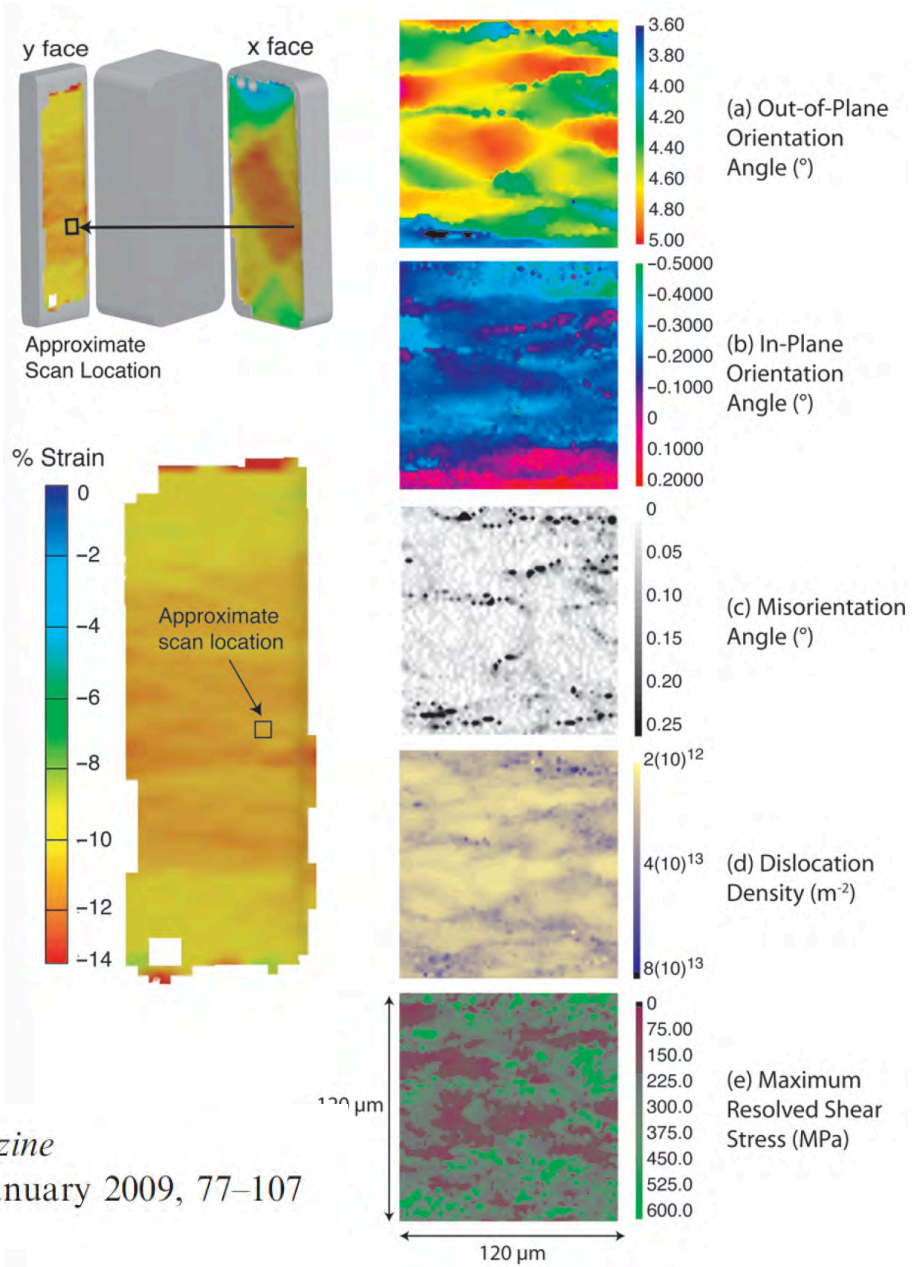

Philosophical Magazine
Vol. 89, No. 1, 1 January 2009, 77–107

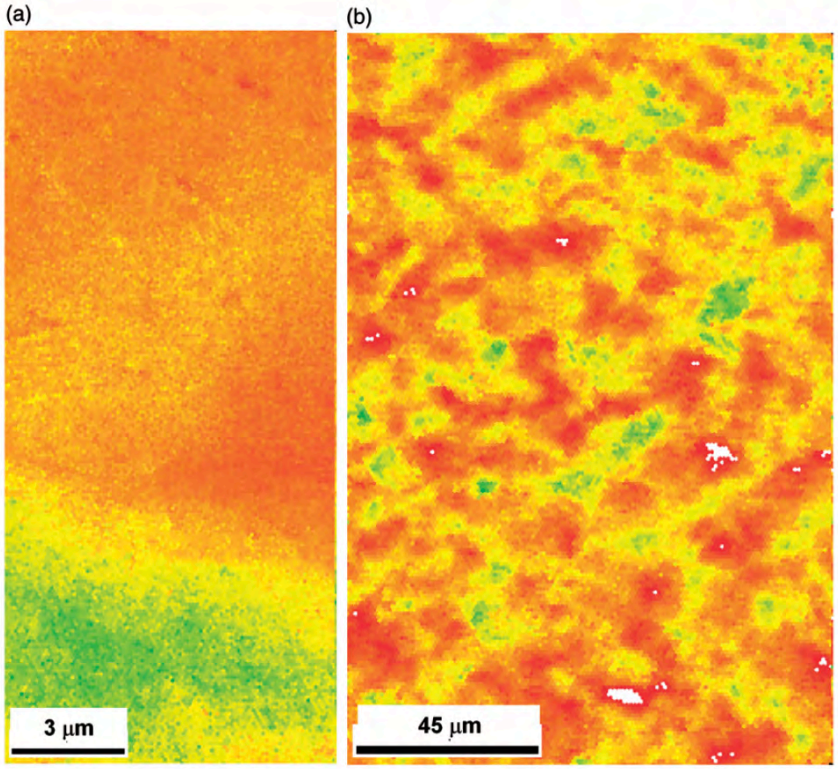

Figure 5. (Colour online). Orientation maps taken at EBSD step sizes of (a) 0.1 µm and (b) 1.0 µm, with the colour scale being the same as that shown in Figure 3a.

Frascati, October 3, 2017

MULTISCALE PHASE SEPARATION

Control and manipulation of multiscale phase separation from

Energy ↑

Atomic scale →
Molecular scale →
Nanoscale →
Mesoscale →
Microscale →

↓ Time

may determine new fundamental material functionality in many challenging open problems in

Energy
Biology & Biomedicine
Technology
Environmental science
Fundamental science
....

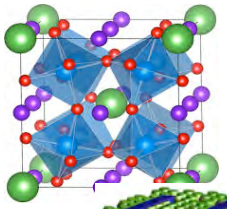

perovskite

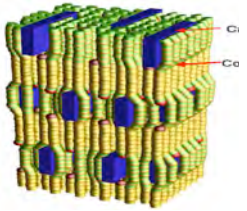

bone

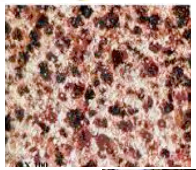

chocolate

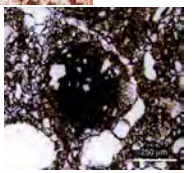

soil

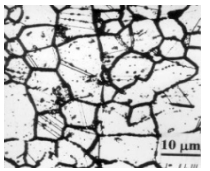

steel

Frascati, October 3, 2017

INFN
Istituto Nazionale di Fisica Nucleare

commentary

Multiscale materials modelling at the mesoscale

Sidney Yip and Michael P. Short

The challenge to link understanding and manipulation at the microscale to functional behaviour at the macroscale defines the frontiers of mesoscale science.

NATURE MATERIALS | VOL 12 | SEPTEMBER 2013 | www.nature.com/naturematerials

Frascati, October 3, 2017

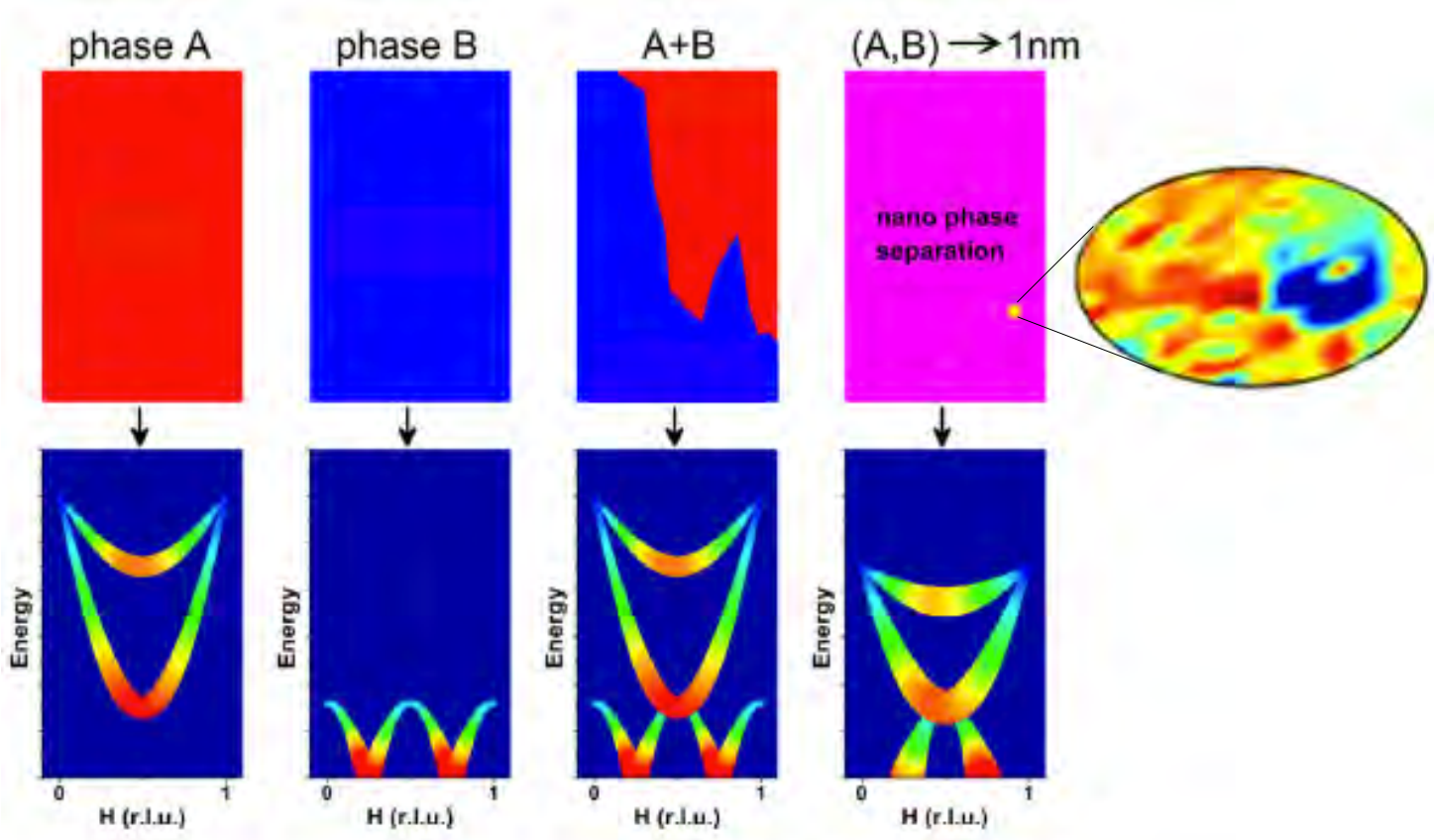

Frascati, October 3, 2017

INFN
Istituto Nazionale di Fisica Nucleare

The new physics of this century is focusing to understand novel intricate non trivial mesoscale inhomogeneity in heterogeneous materials where novel low energy Quantum Physics is emerging.

The mesoscopic world separates the atomic scale (0.1-10 nm) from the macroscopic world (d>100 microns).

Frascati, October 3, 2017

New materials for accelerators

To increase the accelerating gradient of RF cavities working at high frequencies we investigated copper materials coated by Mo via sputtering under vacuum. Structural and electronic characterisation of Mo coatings obtained via the sputtering and annealed up to 600°C have been performed.

This method is a promising approach to obtain homogeneous coatings suitable to increase performances of RF cavities working at high frequencies. We combined FIB imaging to visualise at high spatial resolution the morphology of Mo films and to accurately measure their thickness, with transport experiments to measure the resistivity, while XRD and XAS were used to evaluate the degree of crystallinity, identify different ordered phases and probe the local structure and their electronic properties.

Dedicated RF devices with Mo have been already manufactured at LNF. Mo and Mo oxides with a full characterisation of the conductivity properties are under investigation to optimise manufacturing procedures capable to deposit high-performance coatings.

Why study TMs and TM oxides?

These materials can have unusual and useful electronic and magnetic properties. Many of these properties strongly depend on defects such as vacancies, dislocations, stacking faults, grain boundaries, etc. These "defects" affect the local oxygen bonding.
We can grow films trying to improve functional properties, e.g., working with doping, strain, stress, different kinetics of growth (non-equilibrium processes), annealing, etc.

Can strain/stress effects be correlated with changes in electronic properties (e.g., electronic band structure)?

Can structural parameters (e.g., strain, doping, defects, …) be correlated with changes in magnetic/electronic behaviour?

What type of defects are stable/meta-stable?

Can results be understood in terms of surface chemistry, activity, selectivity, …. etc.?

…..

Frascati, October 3, 2017

Istituto Nazionale di Fisica Nucleare

Qazilbash et al., Nature Phys. 2009

Comparison of various exotic conductors as well as a few conventional metals (Ag and Cu) based on the ratio of the experimental kinetic energy to that calculated within band theory.

These exotic conductors share at least:
a) high-Tc superconductivity
b) itinerant magnetism and/or
c) electronic correlations.

The correlated metal regime is characterized by a substantially reduced empirical kinetic energy of charge carriers compared with theory.
The electron-phonon coupling does not result in a significant reduction of the electron's kinetic energy (unless it is extremely strong as to lead to polaron formation). As an example, the electron-phonon coupling in the MgB_2 superconductor results in $K_{exp}=K_{band}<1$ in the metallic state.

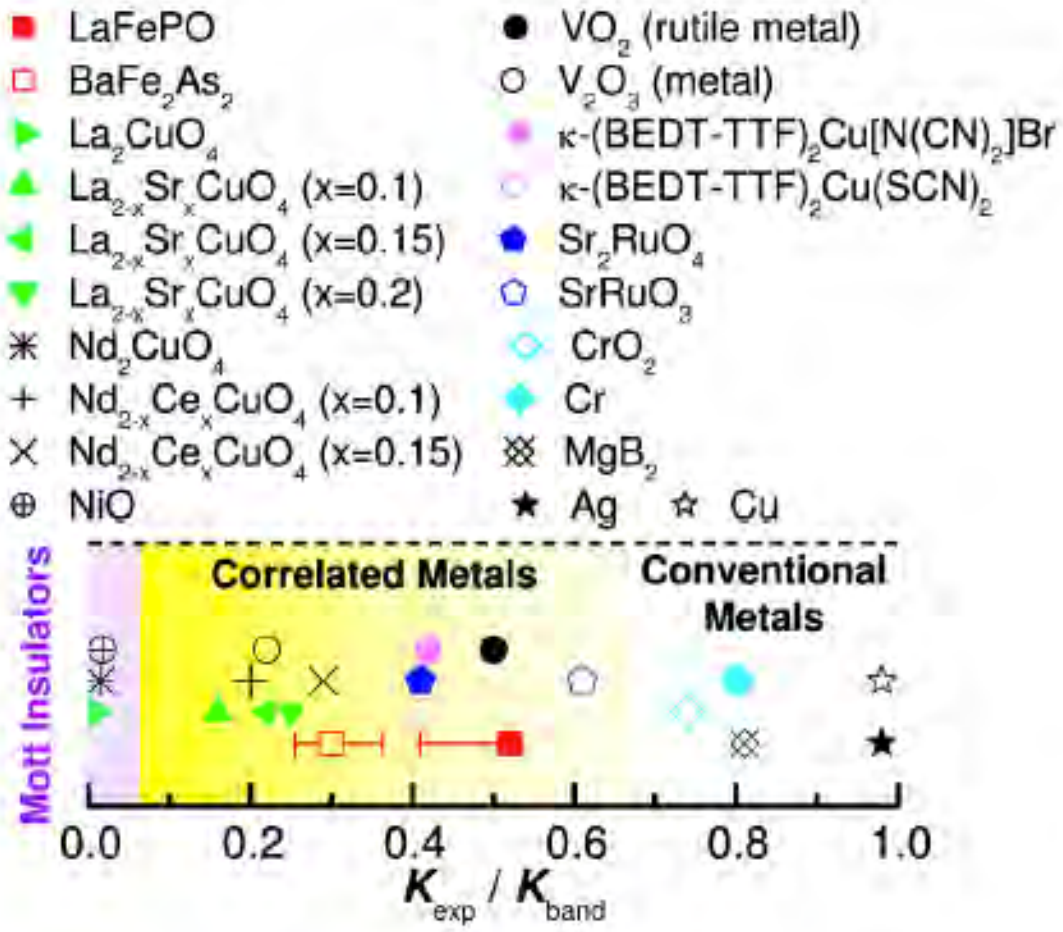

Frascati, October 3, 2017

Mo oxides

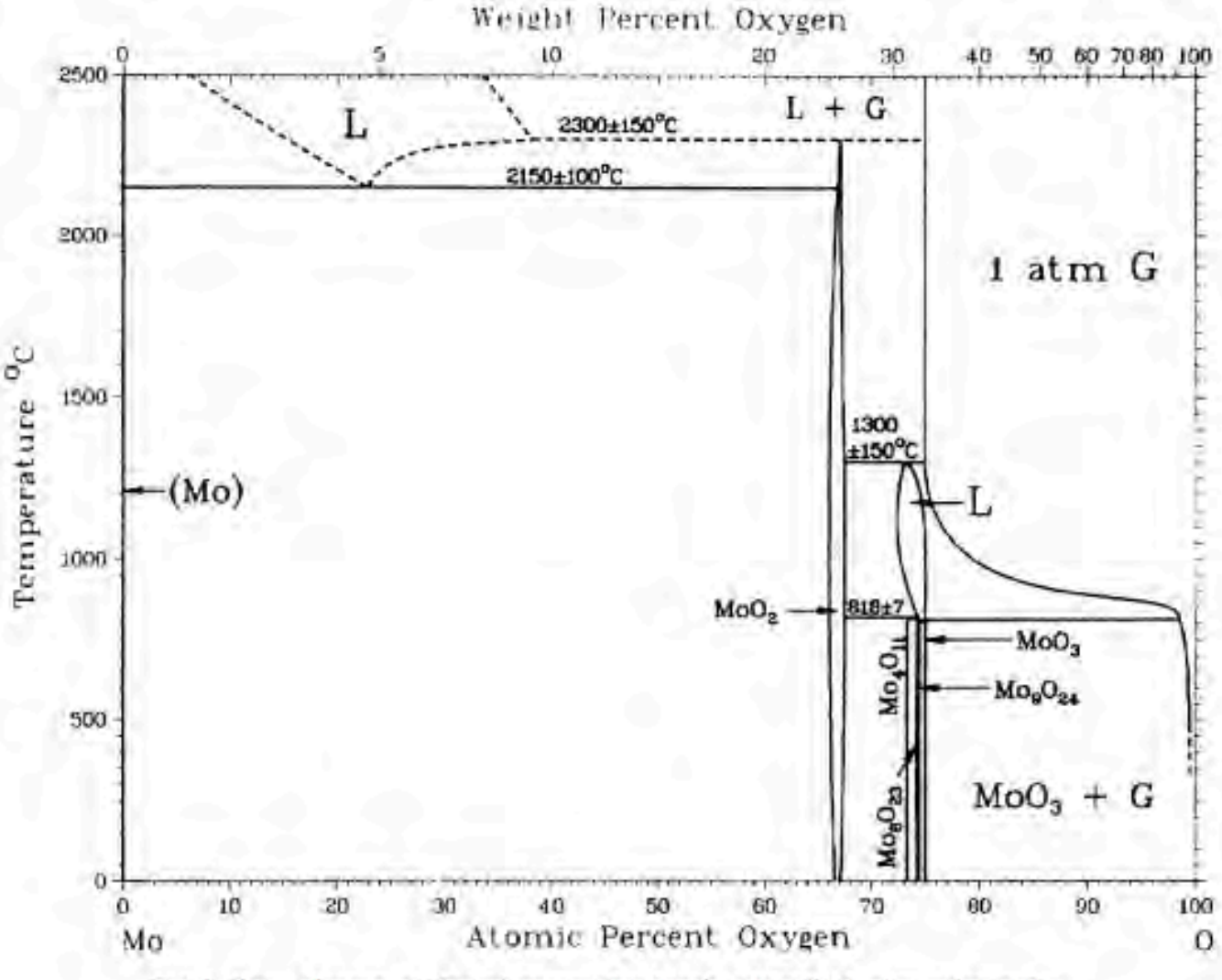

Frascati, October 3, 2017

Mo films

Although the solubility of oxygen in solid Mo is extremely low, the growth of Mo films is strongly affected by the presence of oxygen atoms. Because of the complexity of the phase diagram of the Mo–O system with many phases corresponding to oxide compounds with both transparent and insulating phases, e.g., MoO_3, or metallic phases such as MoO_2, the different films are multiphase systems of high-interest for both fundamental and technological applications.

An extensive literature is available on Mo-based films and coatings and many researches aim to clarify the role of the internal mechanical stress, the impurity concentration, the texture or the surface roughness and their correlation with deposition parameters, such as pressure, DC power or temperature of the substrate. In spite of the data available, due to the presence of different oxide compositions, amorphous phases, microstructure defects and grain size the properties of Mo films is still not clear what is the lowest achievable resistivity of relatively thick films such as those necessary in high gradient accelerating structures (~µm range).

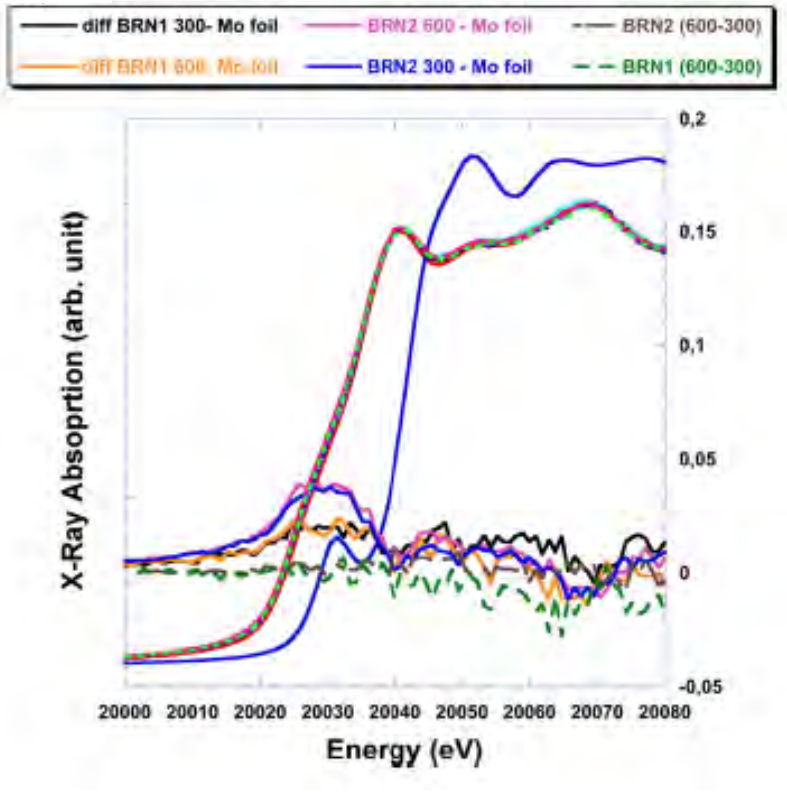

A. Marcelli et al., Surface & Coatings Technology 261 (2015) 391-397

Frascati, October 3, 2017

Experimental methods

Rutherford Backscattering (RBS) data show the elemental profile of Mo coatings.

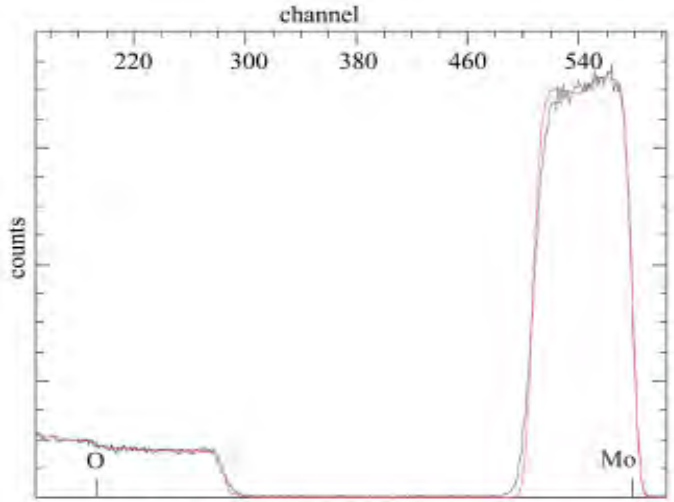

Fig. 12. 2 MeV He (normal incidence, scattering angle 165°) RBS spectrum (black line) obtained on a Mo film deposited on a SiO_2 substrate. The simulation (red line) indicates that the Mo film contains oxygen with a maximum concentration of 25%. The film contains 8.5×10^{17} Mo/cm^2 that corresponds to a Mo coating of about 130 nm thickness. Mo and O surface scattering contributions are reported as green labels.

Mo 3d photoemission (XPS) spectra giving the oxide content in metallic Mo coatings.

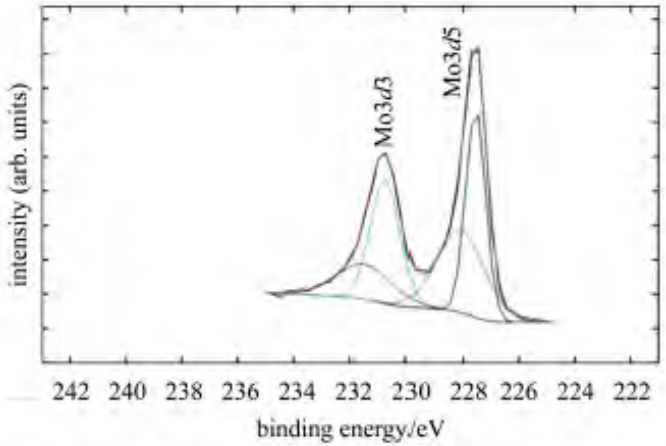

Fig. 14. Deconvolution of the 3d doublet of the molybdenum spectrum. The measured peak (150 nm deep inside the 300 nm film) is well represented by two doublets corresponding to electrons from the 3d shell, the first one at 227.55 in binding energy corresponds to the metallic Molybdenum, the second one at 228.05 shows the typical chemical shift corresponding to the Molybdenum from MoO_2.

S. Bini, et al., Chinese Physics C 37 (2013) 097005-7

Experimental methods

The electrical properties of Mo sputtered coatings have been measured via sample surface impedance probed as a function of the frequency through a Corbino disk geometry with a Vector Network Analyzer Anritsu 37297D. The connection between the cable and the sample was made through a double spring method.

S. Bini, et al., Chinese Physics C 37 (2013) 097005-7

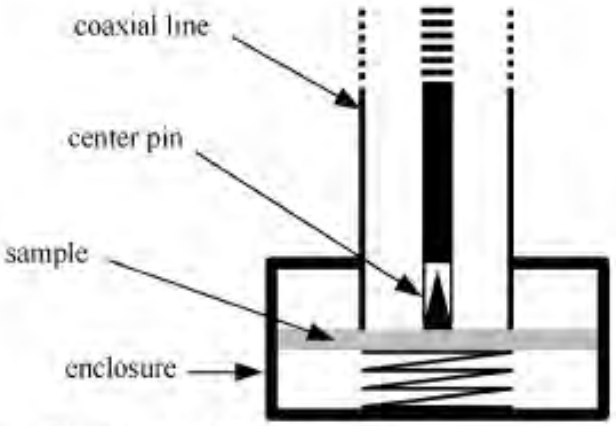

Fig. 5. Sketch of the contact between sample and coaxial line.

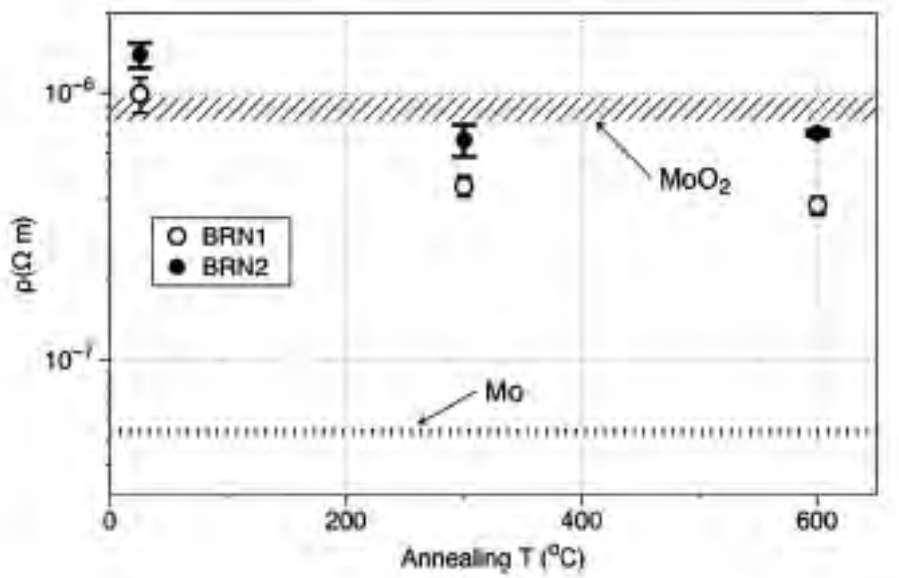

Fig. 2. Resistivity values of BRN1 and BRN2 samples for different annealing temperatures. Mo and MoO_2 values available from the literature are also shown.

In a logarithmic scale we compare the behaviour of the electrical resistivity of some Mo coatings. Although the resistivity values are lower in the thinner sample, after the annealing a clear decrease of the resistivity occurs in both samples, and the observed variation is larger in the ticker samples.

Frascati, October 3, 2017

Experimental methods

To characterise Mo coatings we used a focused ion beam (FIB) microscope.
FIB visualises the coating morphologies at high spatial resolution and allows to measure the thickness of the coating.
A typical FIB image from a Mo film grown on Al_2O_3 (sample B5) is shown on the right. It is characterised by a thickness of ~615 nm. On such coatings we collected XAS spectra at the Mo K edge.

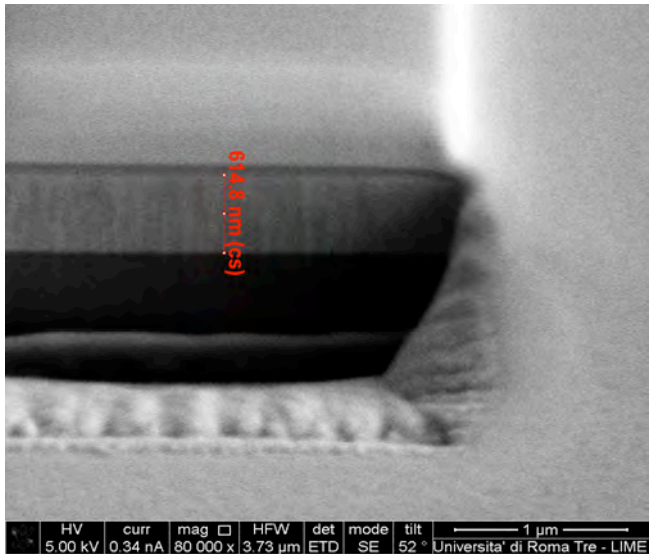

Table 1 Measured thickness of all investigated Mo coatings.

Sample	Mo coatings	Thickness /nm[a]
A1	Mo/ Cu	630
A2	Mo/Cu	1300
B1	Mo/Al_2O_3	70-75
B2	Mo/Al_2O_3	130-140
B3	Mo/Al_2O_3	205-225
B4	Mo/Al_2O_3	310
B5	Mo/Al_2O_3	615
B6	Mo/Al_2O_3	1030

[a]measured with a Focused Ion Beam (FIB)

S. Bini, et al., Chinese Physics C 37 (2013) 097005-7

X-RAY ABSORPTION SPECTROSCOPY

LOCAL AND PARTIAL EMPTY DENSITY OF STATES

CROSS SECTION

$$\sigma(\omega) = 4\pi^2\alpha\hbar\omega \sum_{if} \{|\langle f|\hat{\varepsilon}\cdot\boldsymbol{r}|i\rangle|^2 + (1/4)|\langle f|\hat{\varepsilon}\cdot\boldsymbol{r}\boldsymbol{k}\cdot\boldsymbol{r}|i\rangle|^2\}\delta(E_f - E_i - \hbar\omega).$$

ONLY DIPOLE AND ELECTRIC QUADRUPOLE TERMS ARE CONSIDERED

$$\sigma(\omega) = \sigma_\alpha(\omega)\,[1 + \chi(\omega)] = \sigma_\alpha(\omega) + \sigma_\alpha(\omega)\,\chi(\omega)$$

HOW IT WORKS?

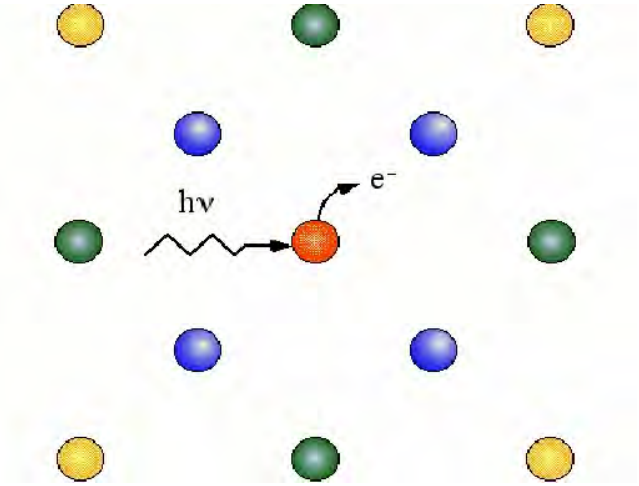

Frascati, October 3, 2017

XANES spectroscopy

Being a fast (10^{-15} s) and local probe (few Å) of a selected atomic species, which also does not require a long range order, XANES spectroscopy represents an almost unique spectroscopic technique. Using extremely small spots, without space averaging, it is suited to investigate the local structure and the electronic properties of different polymorphs, systems with vacancies/impurities/defects, materials where complex magnetic, electronic and structural phase separations occur.

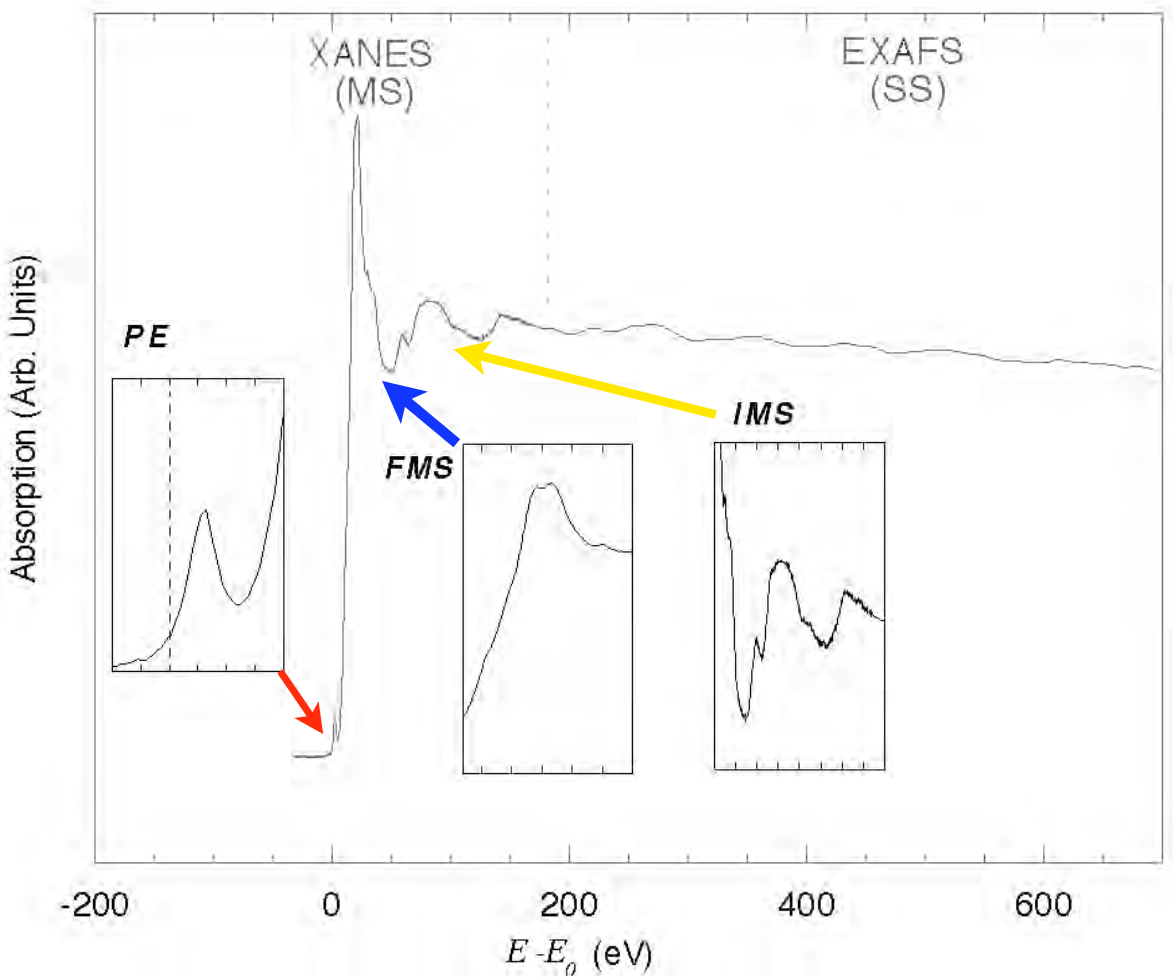

XANES Analysis: Oxidation State

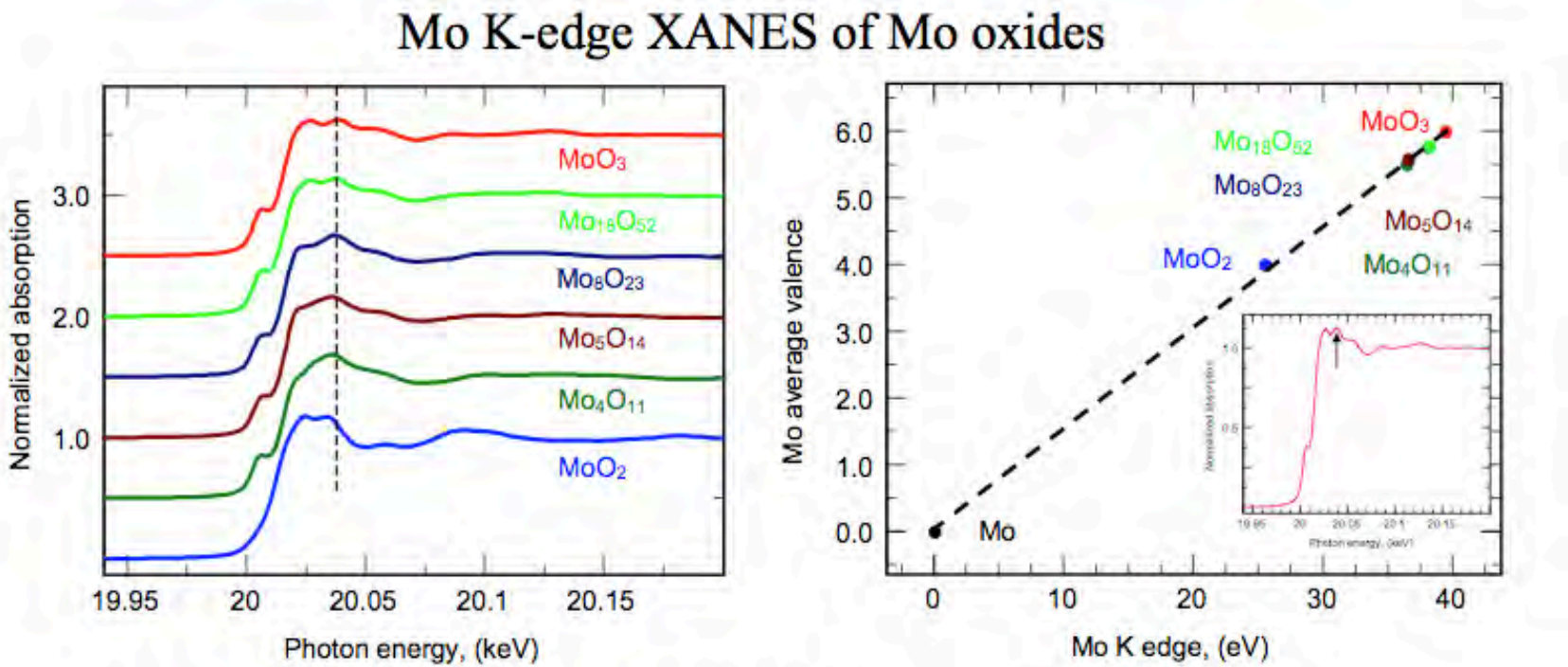

- Linear fit of Mo valence with K-edge position only obtained using a feature above the absorption edge!

T. Ressler et al. J. Cat 210 (2002) 67

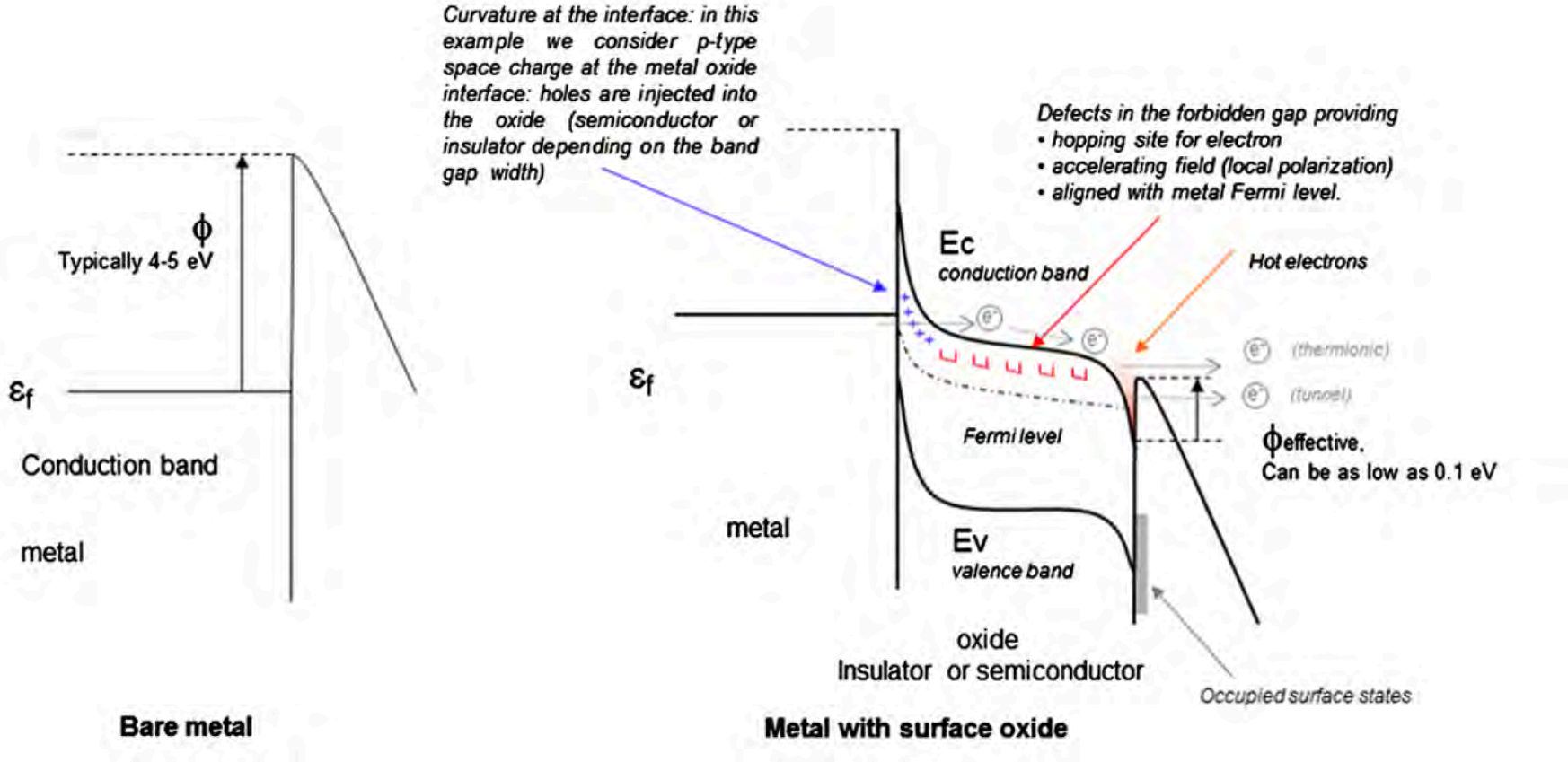

Frascati, October 3, 2017

TM oxides on TM surfaces: Mo on Cu

- calculations of transport properties of coatings of Cu/MoO_3 and alloys such as CuAg/MoO_3, etc. with thickness from few nm to tens of nm;
- growth of oxides films on Cu, CuAg, CuV, etc. metallic surfaces;
- characterization of coatings and oxides materials;
- breakdown tests and of field emission on these surfaces.

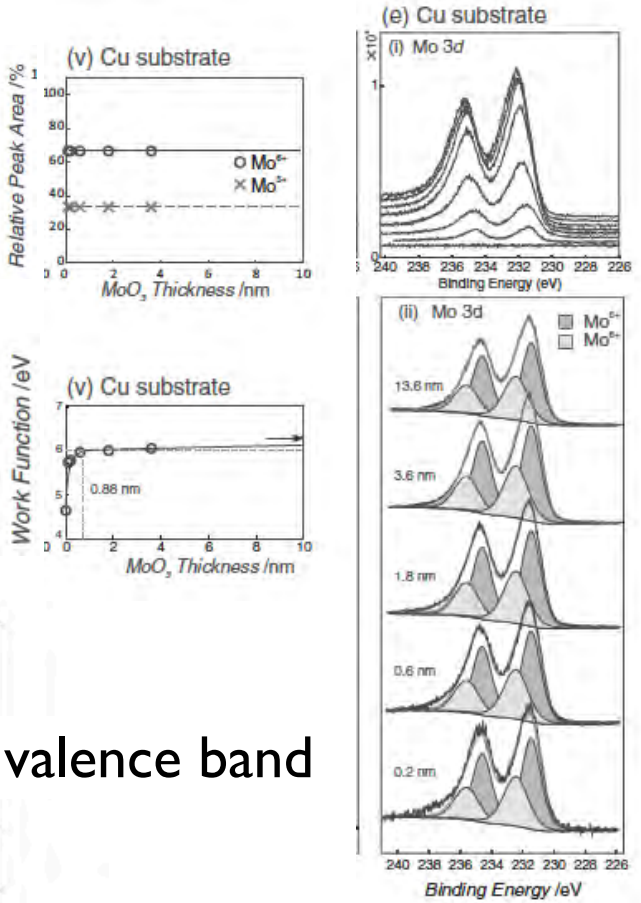

UPS valence band

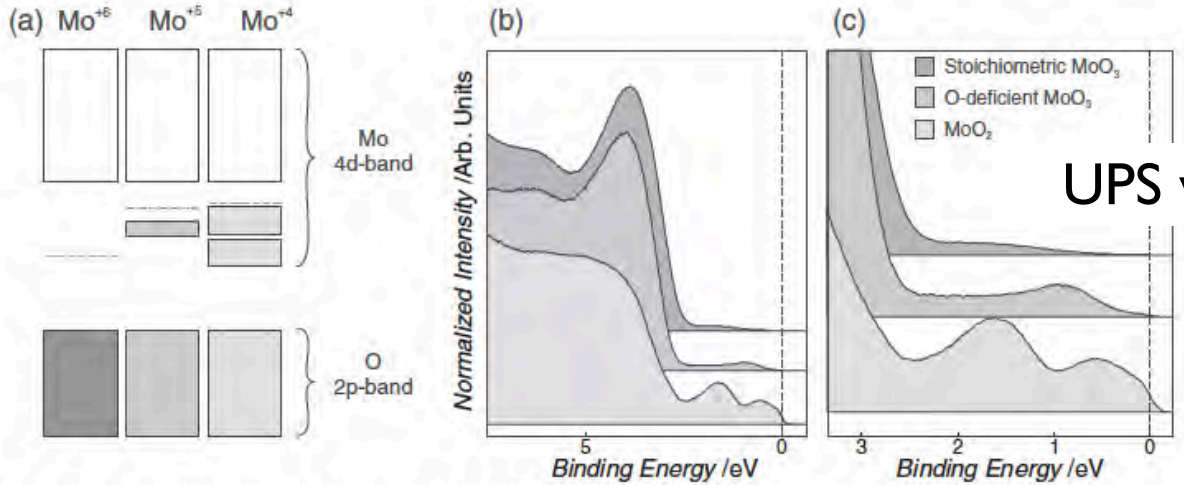

Mark T. Greiner et al. Adv. Funct. Mater. 23, 215 (2013)

Figure 2. a) Schematic energy-level diagram of MoO_3, O-deficient MoO_3, and MoO_2. b) UPS valence band spectra and c) expanded view of the "defect" feature of MoO_3, O-deficient MoO_3 and MoO_2.

New coating materials & methods

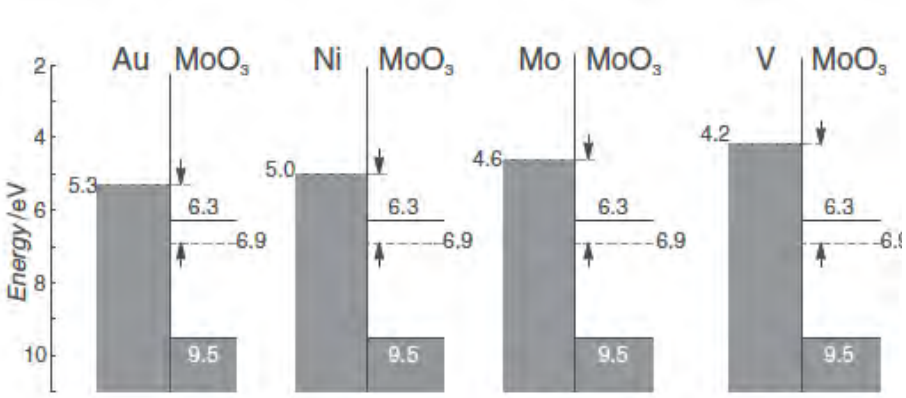

Mark T. Greiner et al. Adv. Funct. Mater. 23, 215 (2013)

XAS experiment on Mo growth on different substrates.

On the left different WFs for MoO_3 on different TMs substrates

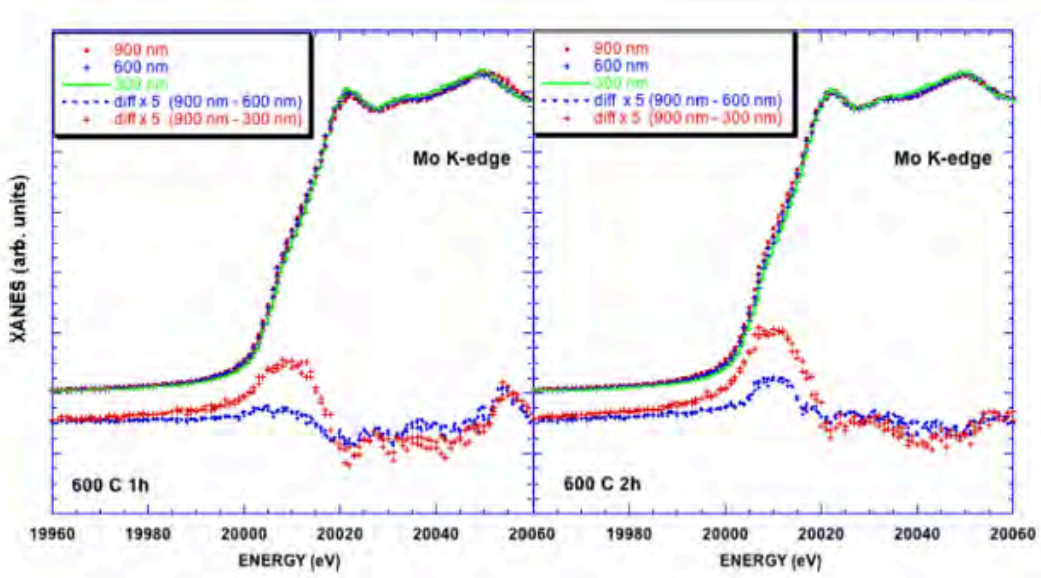

An extensive and accurate characterisation of the conductivity and mechanical properties of Mo and Mo oxides coatings may identify reliable procedures capable to growth stable and hard semi-metallic films with a high work function to reduce the dark current.

Frascati, October 3, 2017

INFN
Istituto Nazionale di Fisica Nucleare

PHYSICAL REVIEW APPLIED **4,** 024015 (2015)

Effects of Surface Nonuniformities on the Mean Transverse Energy from Photocathodes

Siddharth Karkare* and Ivan Bazarov

CLASSE, Cornell University, Ithaca, New York 14853, USA

(Received 24 March 2015; revised manuscript received 29 July 2015; published 24 August 2015)

The performance of photoinjectors is limited by the lowest value of the mean transverse energy of the electrons obtained from photocathodes. The factors that influence the mean transverse energy are poorly understood. In this paper, we develop models to calculate the effect of spatial work-function variations and subnanometer-scale roughness and surface defects on the mean transverse energy. We show that these can limit the lowest value of mean transverse energy achieved and that atomically perfect surfaces will be required to further reduce the mean transverse energy obtained from photocathodes.

DOI: 10.1103/PhysRevApplied.4.024015

JOURNAL OF APPLIED PHYSICS **114,** 243302 (2013)

CrossMark

Local changes of work function near rough features on Cu surfaces operated under high external electric field

Flyura Djurabekova,[1,a)] Avaz Ruzibaev,[1] Eero Holmström,[2,3] Stefan Parviainen,[1] and Mikko Hakala[2]

[1]*Helsinki Institute of Physics and Department of Physics, University of Helsinki, P.O. Box 43, FI-00014 Helsinki, Finland*

[2]*Department of Physics, University of Helsinki, P.O. Box 64, FIN-00014 Helsinki, Finland*

[3]*Department of Earth Sciences, Faculty of Maths and Physical Sciences, UCL Earth Sciences, Gower Street, London WC1E 6BT, United Kingdom*

(Received 30 October 2013; accepted 9 December 2013; published online 30 December 2013)

"The change in the value of the work function indicates the strong influence of intrinsic defects on this parameter, which requires further investigation. Moreover, we were able to validate the approach which we developed previously for the dynamic simulation of the effect of electric field on extended metal surfaces."

Frascati, October 3, 2017

INFN Istituto Nazionale di Fisica Nucleare

LABORATORI NAZIONALI DI FRASCATI
SIDS-Pubblicazioni

INFN-17-13/LNF
May 6, 2017

Characterization of the transport properties of MoO_3 films on copper

C. Bonavolontà[1)], M. Valentino[1,2)], M. de Lucia[1)], M. Ambrosio[1)], C. Aramo[1)], S. Macis[3)], I. Davoli[3)], G. Castorina[4,5)], F. Monforte[6)], B. Spataro[4)], M. Scarselli[3)], S. Lupi[7)] and A. Marcelli[4,8)]

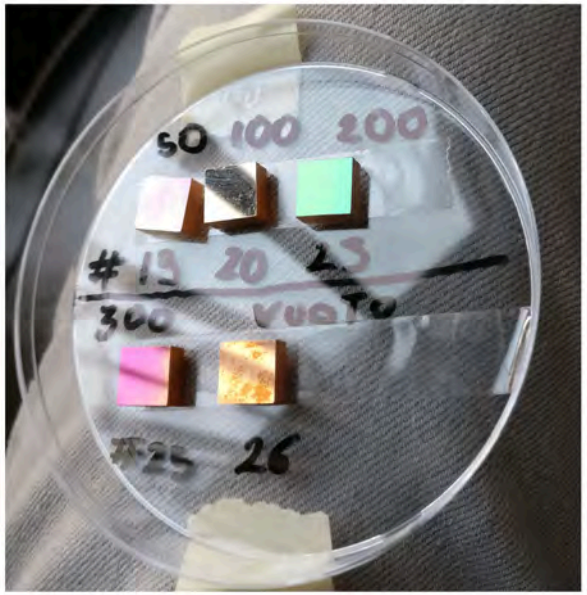

Figure 2: Photograph showing evaporated samples of MoO_3 on copper. Due to the different thickness, each film can be easily recognized by its different colour.

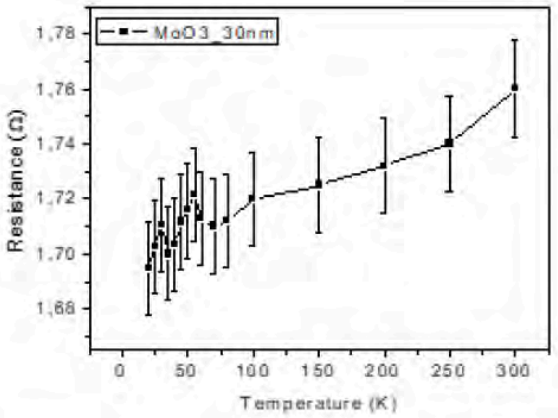

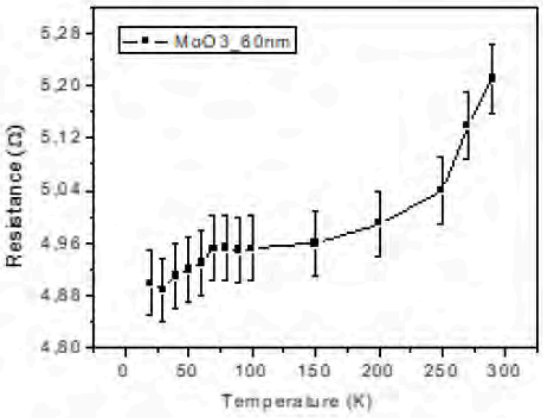

Figure 5: Electrical resistance vs. temperature for MoO_3 samples with thickness: 30 nm (left) and 60 nm (right).

Thin films are conductive and the resistance decreases at low temperature.

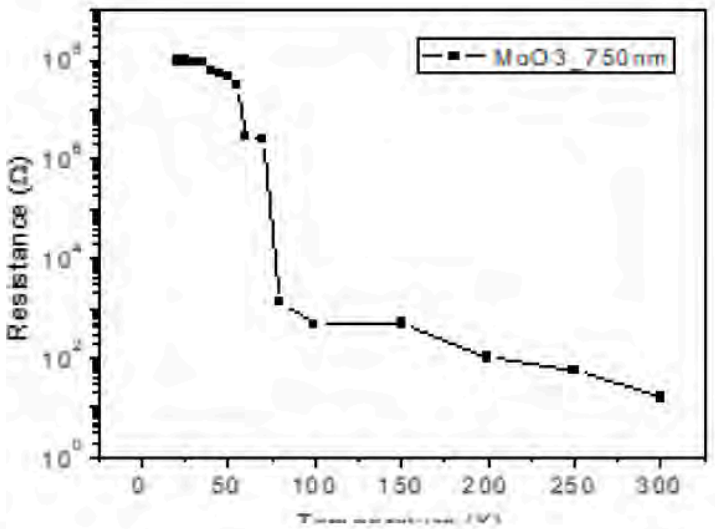

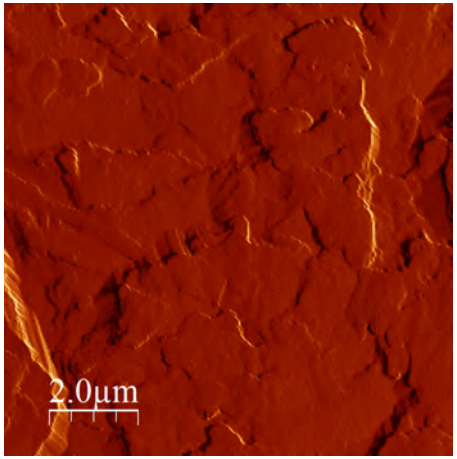

Frascati, October 3, 2017

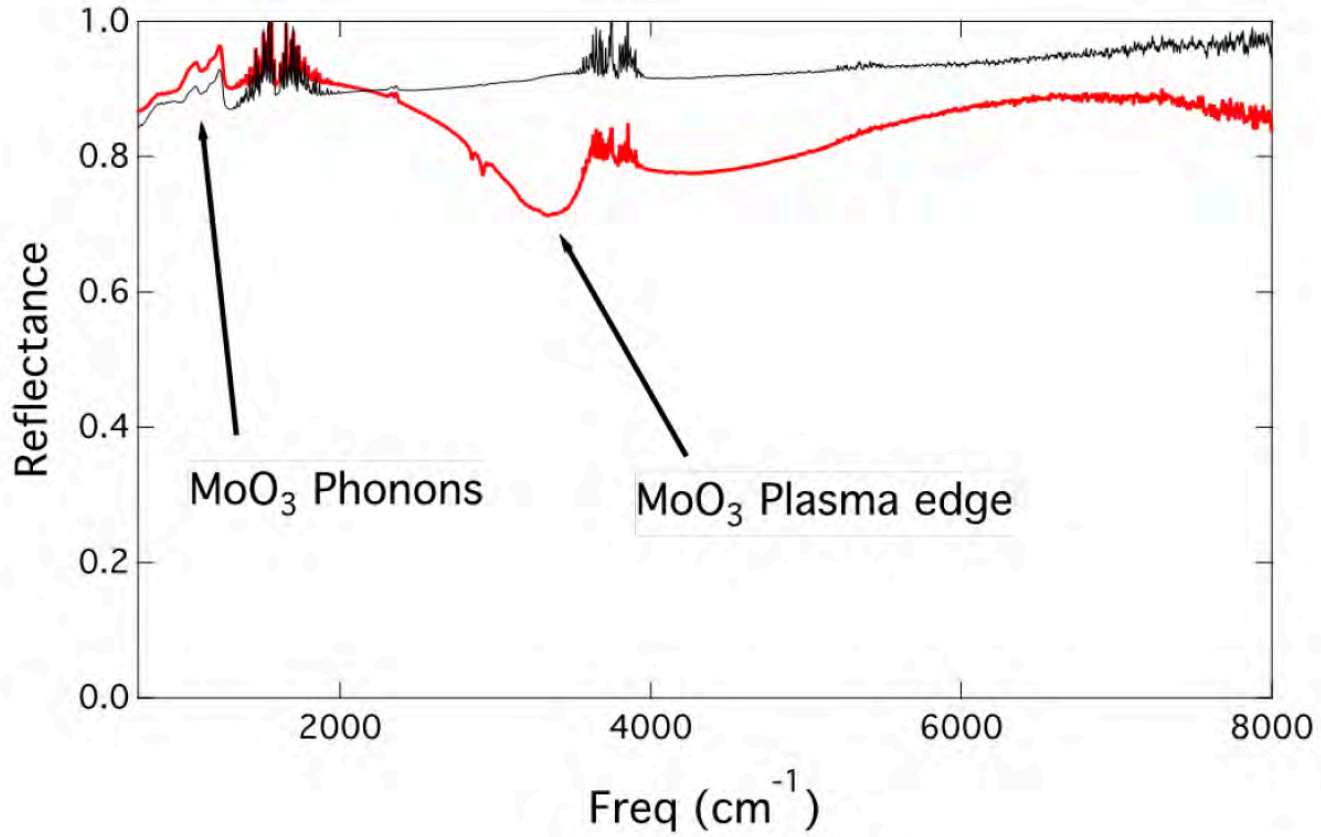

Figure 12: Comparison of the absolute reflectance of MoO_3 films of 30 and 300 nm thickness. While the thinner film shows, at room temperature, a metallic behaviour with a well evident plasma edge in the mid-infrared region, the 300 nm thick film shows an insulating behaviour with a flat (<1) reflectance. The narrow peaks around 1600 and 3900 cm^{-1} are due to the water vapour absorption in the spectrometer.

XAS of Mo coatings

XAS (X-ray Absorption Spectroscopy) is a well-established technique for a direct quantitative measurement of local structure properties such as geometry and coordination numbers in ordered and disorder systems such as coatings or interface. To characterise the chemical status of Mo atoms in our coatings we performed XAS experiments at the Mo K edge at B18, Core XAS beamline at the Diamond Light Source (UK).

Data were collected with focusing radiation in a spot of ~200x200 μm^2 in the fluorescence mode. Experiments have been performed both at normal incidence and at grazing incidence to enhance the signal associated to thin surface layers and in different areas of the Mo coatings.

Frascati, October 3, 2017

condensed matter

MDPI

Article

Materials and Breakdown Phenomena: Heterogeneous Molybdenum Metallic Films

Augusto Marcelli [1,2,3,*], Bruno Spataro [1], Giovanni Castorina [1,4], Wei Xu [2,5], Stefano Sarti [6], Francesca Monforte [7,8] and Giannantonio Cibin [9]

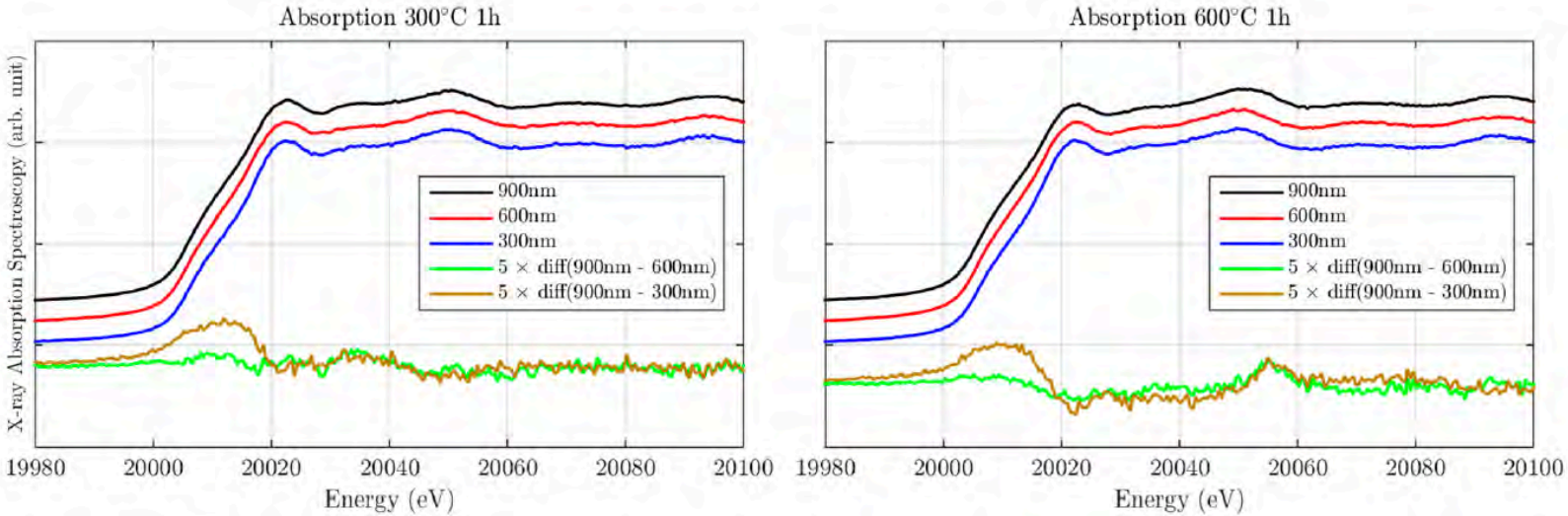

Figure 2. (**Left panel**) comparison of Mo K-edge spectra of samples of 300 nm, 600 nm, and 900 nm annealed at 300 °C for 1 h. The bottom curves are the differences between spectra of different thickness (multiplied 5×); (**Right panel**) the same as in the left panel for the samples with the same thickness, but annealed at 600 °C for 1 h.

Frascati, October 3, 2017

Mo K edge XANES

Comparison of XANES spectra of Mo coatings (top right). Spectra measured in the transmission geometry point out that all coatings has a slightly disordered structure with a negligible Mo oxide contribution. Coatings are similar except for the thick A2 sample (i.e., Mo/Cu) which has a significant Mo oxide contribution.
In the bottom right we plot the edge energy vs. thickness where the Mo K-edge has been determined from the normalized absorption at the height of 0.8. The edge of samples grown on Al_2O_3 (B1-B6) shift vs. thickness due to the changes of the Fermi energy. For samples grown on Cu (A1-A2), XANES spectra are slightly different (in particular the ticker one). Mo coatings are all characterized by a linear expansion of the next-nearest distances around the Mo atoms that clearly depends by the thickness.

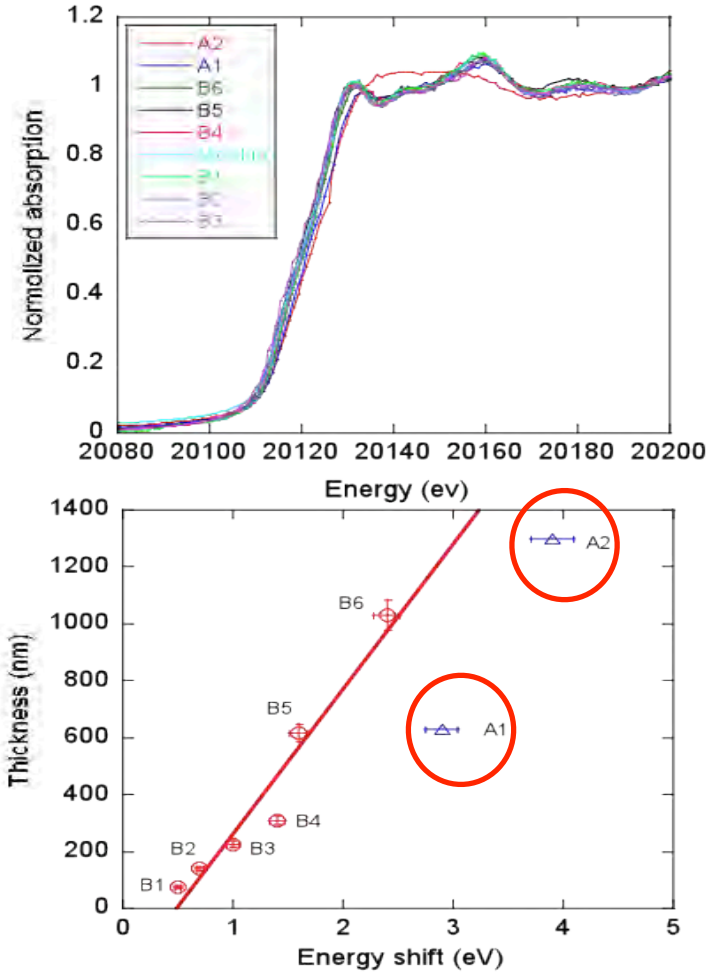

A. Marcelli, B. Spataro, S. Sarti, et al. Characterization of thick conducting molybdenum films: enhanced conductivity via thermal annealing, Surface & Coatings Technology 261, 391 (2015)

S. Bini, B. Spataro, A. Marcelli, S. Sarti, et al., Molybdenum sputtering film characterization for high gradient accelerating structures, Chinese Physics C 37, 097005 (2013)

Y. Xu, B. Spataro, S. Sarti, et al., Structural and morphological characterization of Mo coatings for high gradient accelerating structures, Journal of Physics: Conference Series 430, 012091 (2013)

Frascati, October 3, 2017

Mo K edge XANES

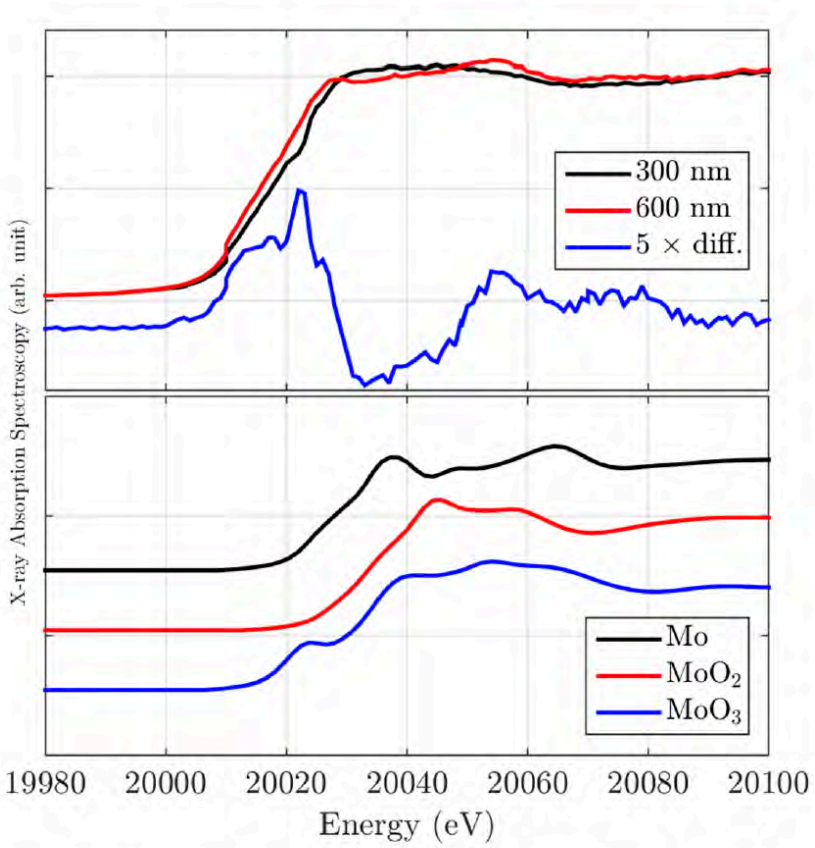

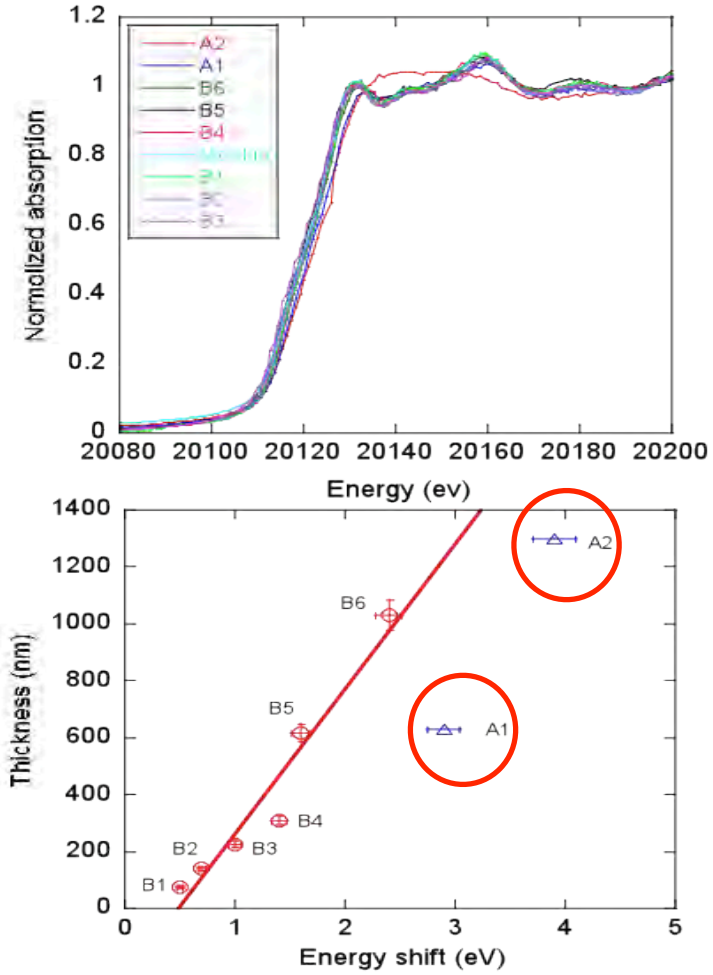

Figure 3. (**Top panel**) comparison of Mo K-edge XANES spectra of two Mo films: 300 nm and 600 nm thick grown on OFHC copper substrates. The blue curve is the difference between the two experimental spectra multiplied by five to enhance the difference at the edge (see text); (**Bottom panel**) comparison among Mo K-edge XANES spectra of Mo metal (black), MoO_2 (red), and MoO_3 (blue) simulated using the full multiple scattering (FMS) theory (see text).

Frascati, October 3, 2017

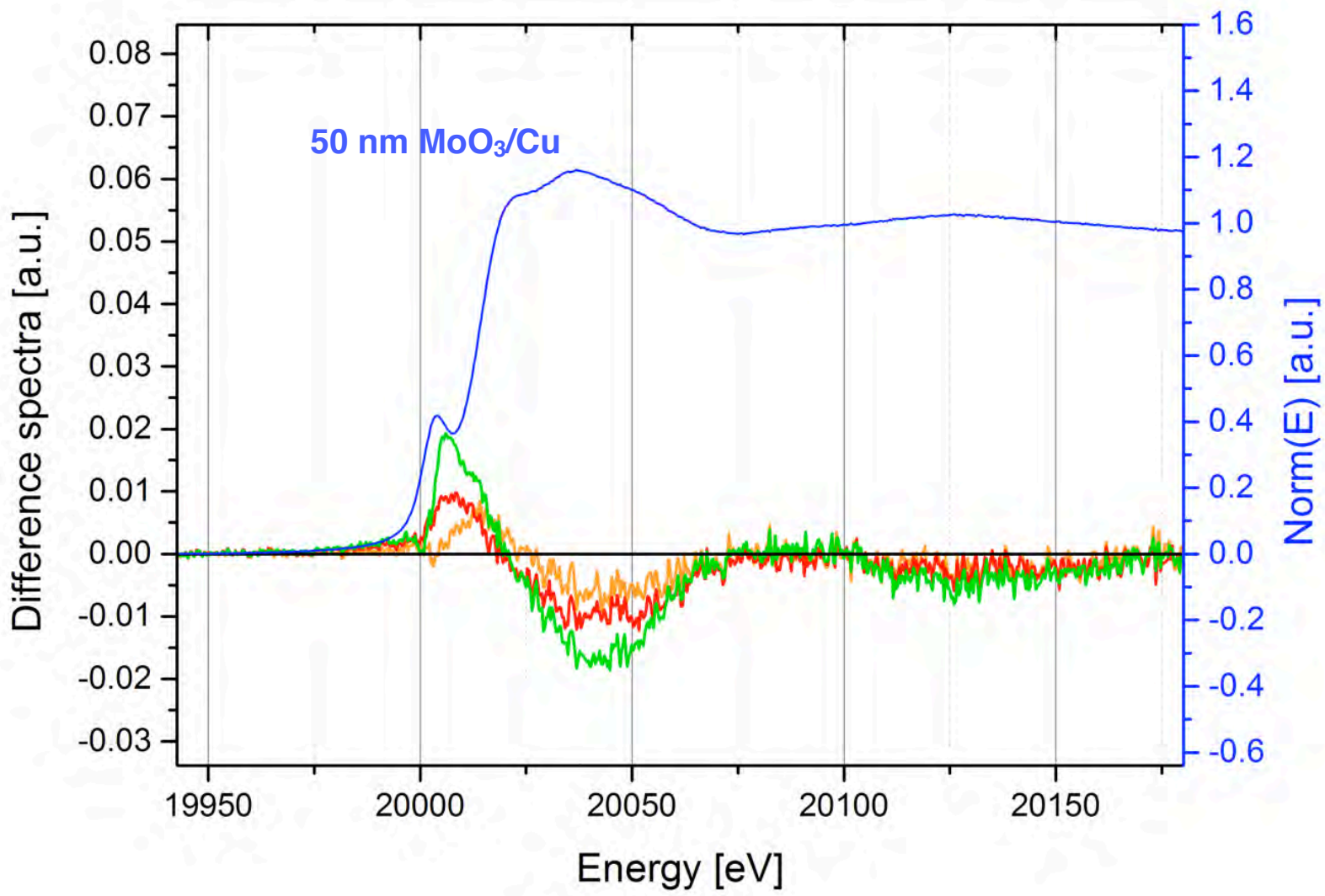

XAS(100nm-50nm)

XAS(200nm-50nm)

XAS(300nm-50nm)

Marcelli, Macis, Spataro et al. unpublished

Frascati, October 3, 2017

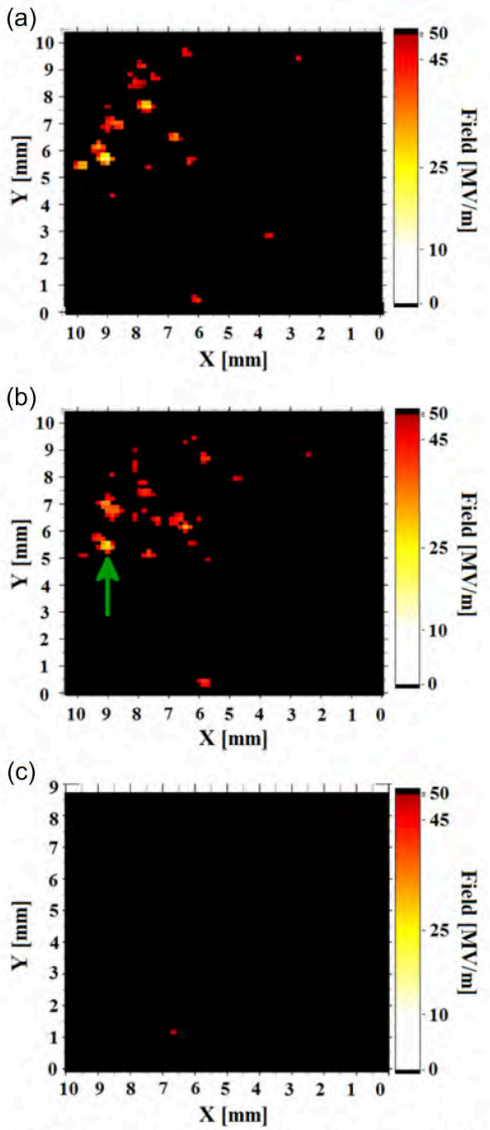

Fig. 4. FE maps up to $E = 50$ MV/m of the single crystal Mo sample after HT at 500 °C (a) and 600 °C (b) and of the much better cleaned polycrystalline sample after HT at 600 °C (c).

Eur. Phys. J. Appl. Phys. (2015) 70: 21301
DOI: 10.1051/epjap/2015150167

THE EUROPEAN PHYSICAL JOURNAL APPLIED PHYSICS

Regular Article

Prevention of electron field emission from molybdenum substrates for photocathodes by the native oxide layer

Stefan Lagotzky[1,a], Roman Barday[2], Andreas Jankowiak[2], Thorsten Kamps[2], Carola Klimm[2], Jens Knobloch[2], Günter Müller[1], Boris Senkovskiy[3], and Frank Siewert[2]

[1] Bergische Universität Wuppertal, FB C Abteilung Physik, Gauss-Str. 20, 42097 Wuppertal, Germany
[2] Helmholtz-Zentrum Berlin für Materialien und Energie GmbH, Hahn-Meitner-Platz 1, 14109 Berlin, Germany
[3] Institut für Festkörperphysik, TU Dresden, 01069 Dresden, Germany

Received: 20 March 2015 / Accepted: 21 April 2015
Published online: 25 May 2015 – © EDP Sciences 2015

FE maps up to E = 50 MV/m on the single crystal Mo sample after HT at 500∘C (a) and 600∘C (b) and of the much better cleaned polycrystalline sample after HT at 600∘C (c).
Well-polished and dry-ice cleaned Mo samples with native oxide did not show parasitic FE up to a field level of 50 MV/m required for photoinjector cavities.
No FE was observed after HT up to 400 ∘C, but 19 (26) emitters occurred after HT at 500 (600)∘C as shown on the left.

Frascati, October 3, 2017

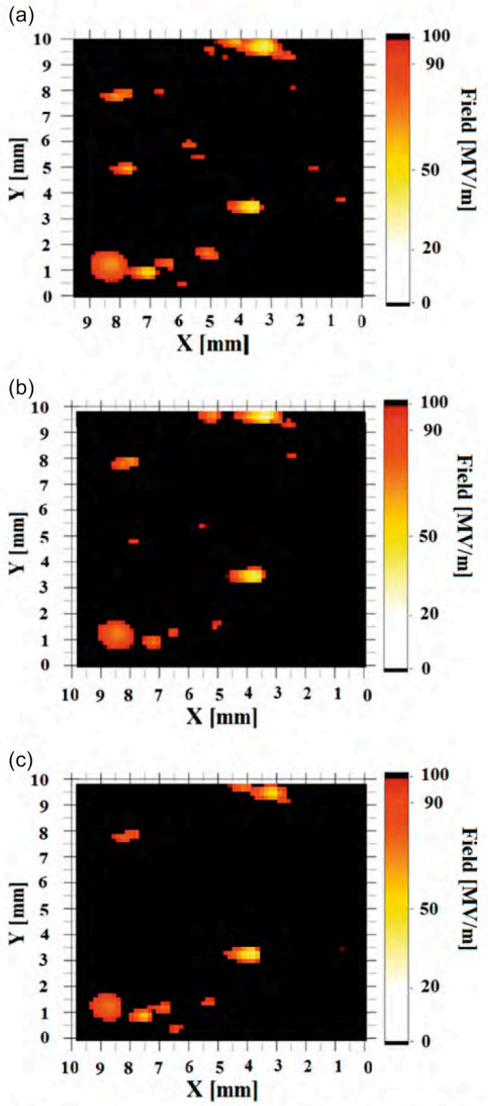

Fig. 6. FE maps of the polycrystalline Mo sample up to $E = 100$ MV/m after HT at 600 °C (a) and after different reoxidation steps with O_2 pressure: $p = 10^5$ Pa at 25 °C (b) and $p = 1$ Pa at 400 °C (c).

…. the same polycrystalline Mo sample was scanned up to 100 MV/m to enhance its FE significantly. Beside both formerly present emitters, about 18 additional ones with E_{on} values of 30–90 MV/m could be activated now as shown in Figure 6a.

It is remarkable that some new emitter show rather low values for E_{on} now. This well-known activation effect for field emitters is usually explained by the creation of conducting channels in the insulating oxide layer ……

Eur. Phys. J. Appl. Phys. (2015) 70: 21301
DOI: 10.1051/epjap/2015150167

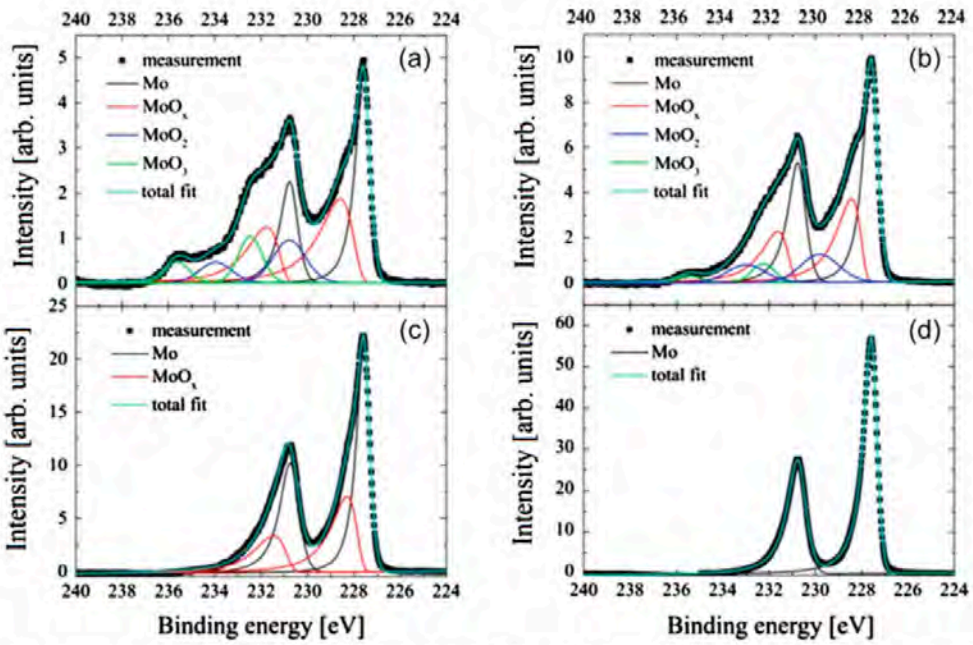

Fig. 11. Mo 3*d* photoemission spectra after HT at 100 °C (a), 300 °C (b), 400 °C (c) and 600 °C (d).

After the XPS measurement the sample was moved into a preparation chamber for a HT. Four treatment cycles were performed in situ with increasing temperature of 100, 300, 400 and 600∘C for 1 h. After each treatment step the sample was transferred back into the analyzing chamber for the XPS measurement.

The position of the illuminated area remains unchanged. The weight *f* for MoO_3 reduces from ~0.33 for the unannealed sample to 0.05 after HT at 300–600∘C.

After HT at 400∘C the molybdenum trioxide layer is dissolved into the bulk (Fig. 11). After the last HT at 600∘C all Mo oxide correlated peaks disappeared, indicating that the oxide film was removed completely.

Eur. Phys. J. Appl. Phys. (2015) 70: 21301
DOI: 10.1051/epjap/2015150167

Istituto Nazionale di Fisica Nucleare

Scale-free structural organization of oxygen interstitials in La_2CuO_{4+y}

Michela Fratini[1]†, Nicola Poccia[1], Alessandro Ricci[1], Gaetano Campi[1,2], Manfred Burghammer[3], Gabriel Aeppli[4] & Antonio Bianconi[1]

NATURE|Vol 466|12 August 2010

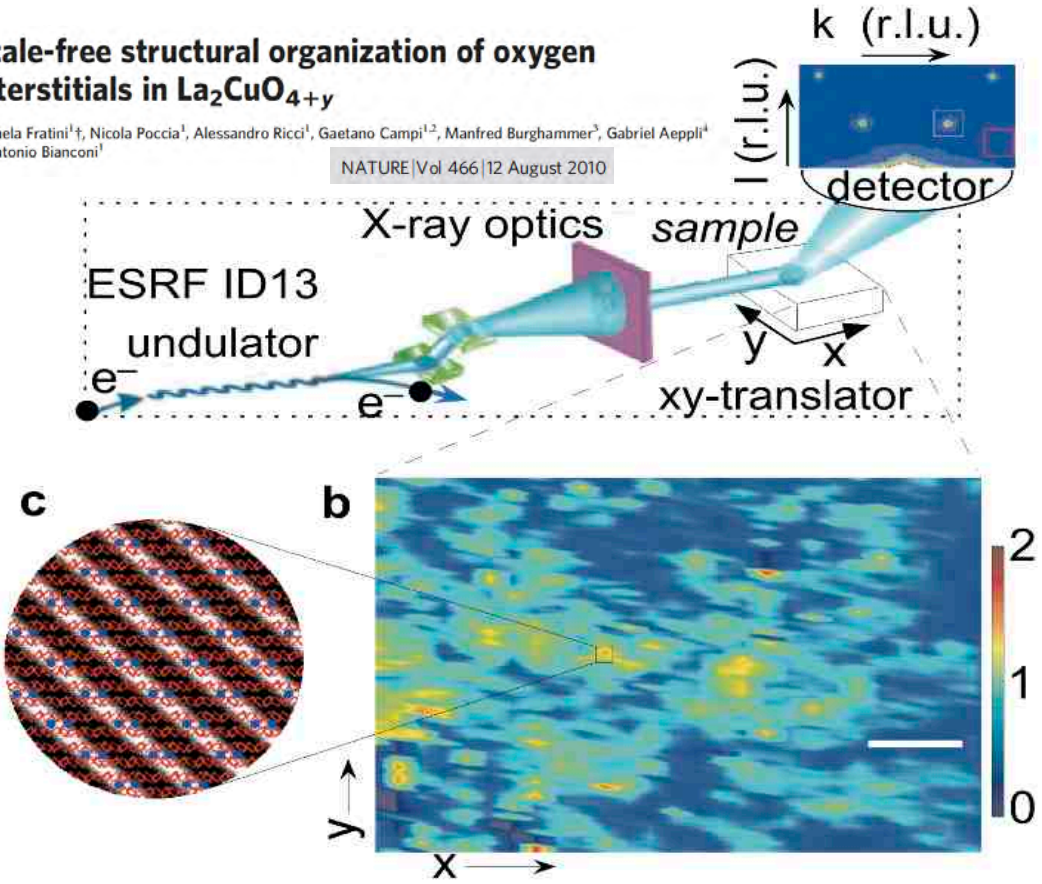

Frascati, October 3, 2017

Even in optimal superconducting samples the oxygen defect order can be highly inhomogeneous. Actually, the glue regions contain incommensurate modulated local lattice distortions, whose spatial extent is most pronounced for the best superconducting samples. For an underdoped single crystal with mobile oxygen interstitials in the spacer La_2O_{2+y}, the incommensurate modulated local lattice distortions form droplets anti-correlated with the ordered Oi. In the simplest among high temperature superconductors, two networks of ordered defects coexist. They can be tuned to achieve optimal superconductivity.
Actually, for a given stoichiometry, the highest transition temperature is obtained when both the ordered oxygen (Oi) and the lattice defects (LLD) form fractal patterns.

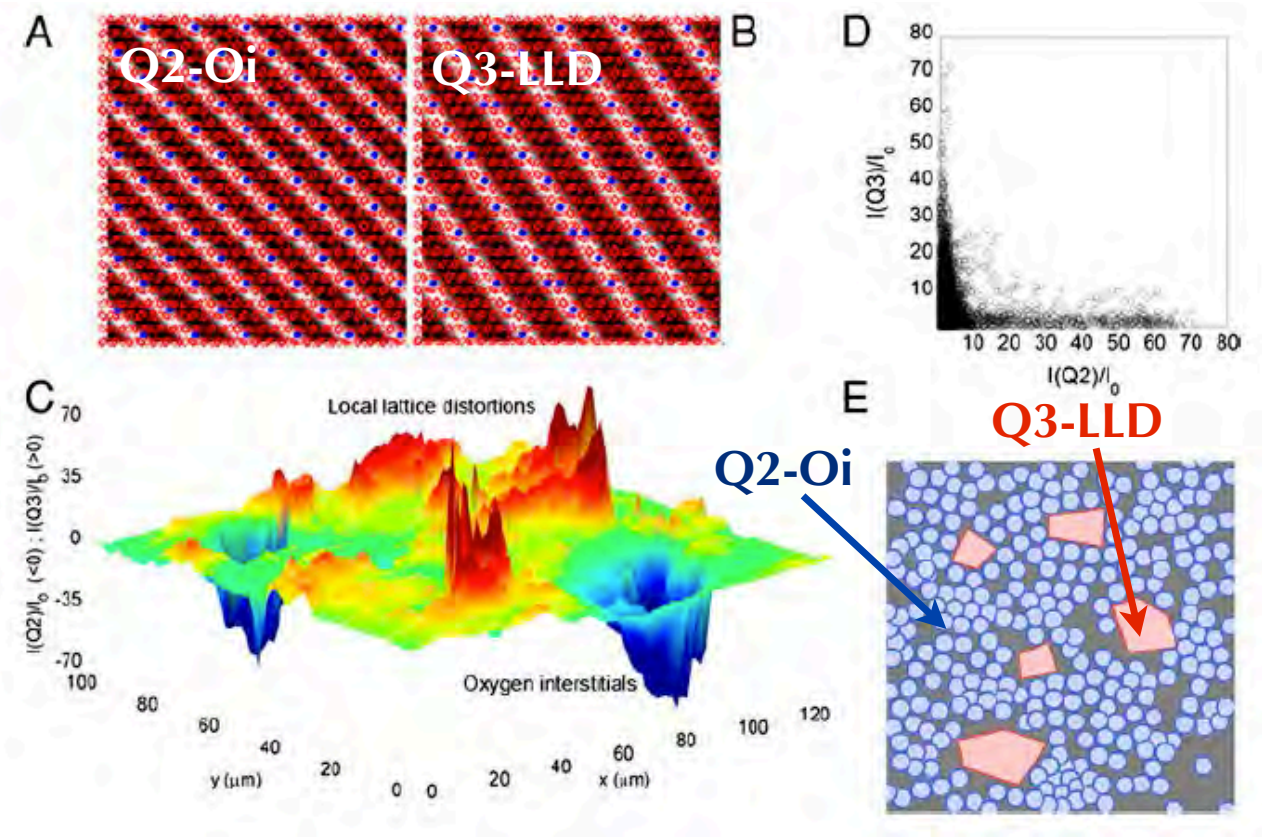

Optimum inhomogeneity of local lattice distortions in La_2CuO_{4+y}

Nicola Poccia[a,b], Alessandro Ricci[a,c], Gaetano Campi[d], Michela Fratini[a,e], Alessandro Puri[f], Daniele Di Gioacchino[f], Augusto Marcelli[f], Michael Reynolds[b], Manfred Burghammer[b], Naurang Lal Saini[a], Gabriel Aeppli[g], and Antonio Bianconi[a,h,i,1]

PNAS | September 25, 2012 | vol. 109 | no. 39 | 15685–15690

Frascati, October 3, 2017

N. Poccia, M. Chorro, A. Ricci, Wei Xu, A. Marcelli, G. Campi and A. Bianconi
Percolative superconductivity in $La_2CuO_{4.06}$ by lattice granularity patterns with scanning micro x-ray absorption near edge structure
Applied Physics Letters 104, 221903 (2014)

µ-XANES measurements were performed using LUCIA at SOLEIL with the high brilliance (1.6 10^{11} ph/s/400 mA) Apple II-UH52 undulator soft X-rays source (0.8–8 keV). The polarized monochromatic photon beam was focused with a couple of KB mirrors on a 2.5 x2.5 µm² spot. At each x-z position, the lanthanum L_3-edge XANES signal was recorded in the fluorescence mode with a 4 elements Si drift Bruker detector.

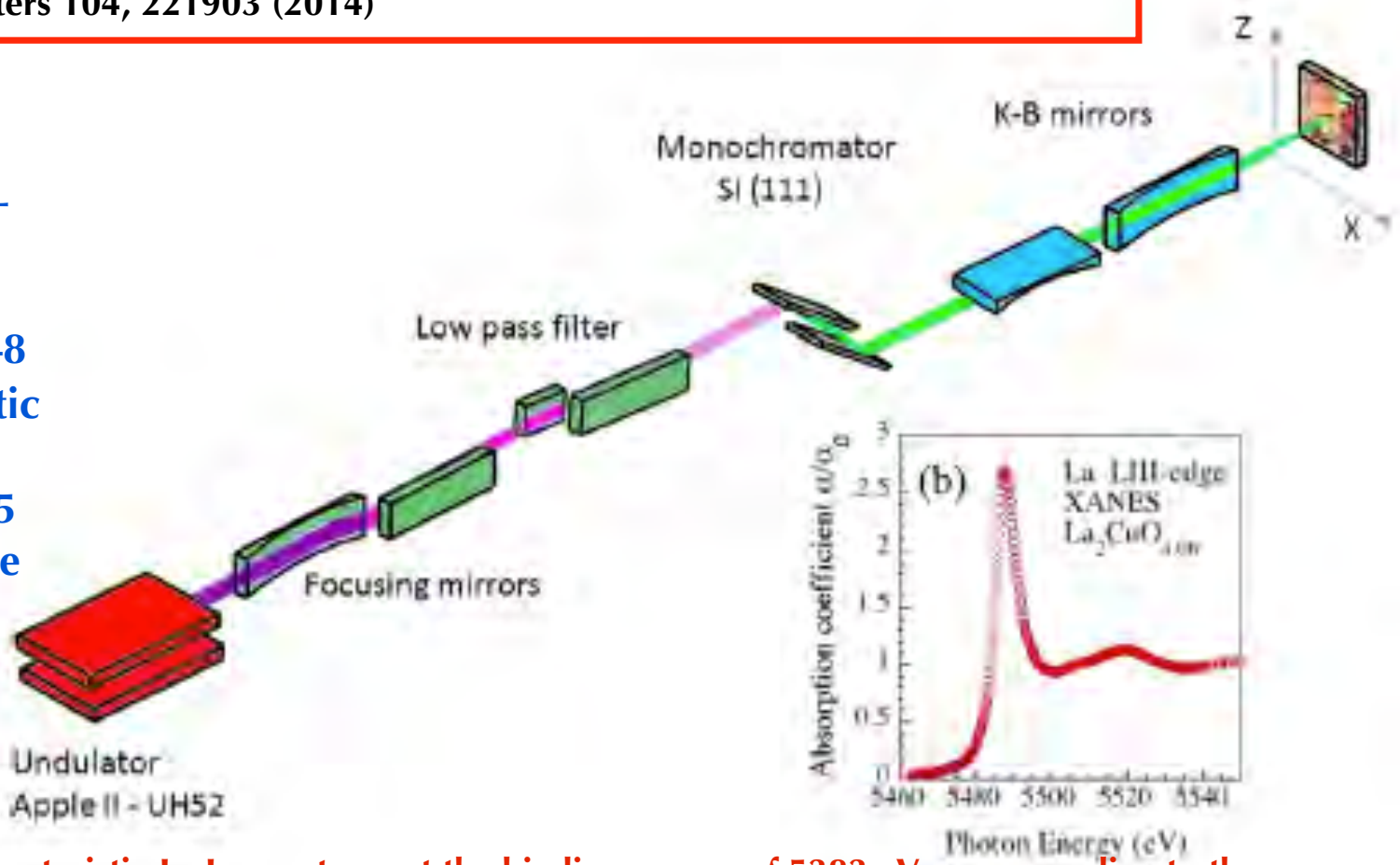

Characteristic La L_3 spectrum at the binding energy of 5383 eV corresponding to the electronic transition from the 2p level to 5d empty states.

Frascati, October 3, 2017

The atomic cluster (~8 Å) surrounding La (green) in a La_2CuO_{4+y} crystal that determines the shape resonance in the La L_3-XANES. The photoelectron wave emitted by the absorbing atoms are scattered by Cu (blue), oxygens (red) and other La ions. In oxygen rich puddles (as in the $La_2CuO_{4.125}$ crystal) the cluster includes additional Oi (purples spheres indicated by the arrows).

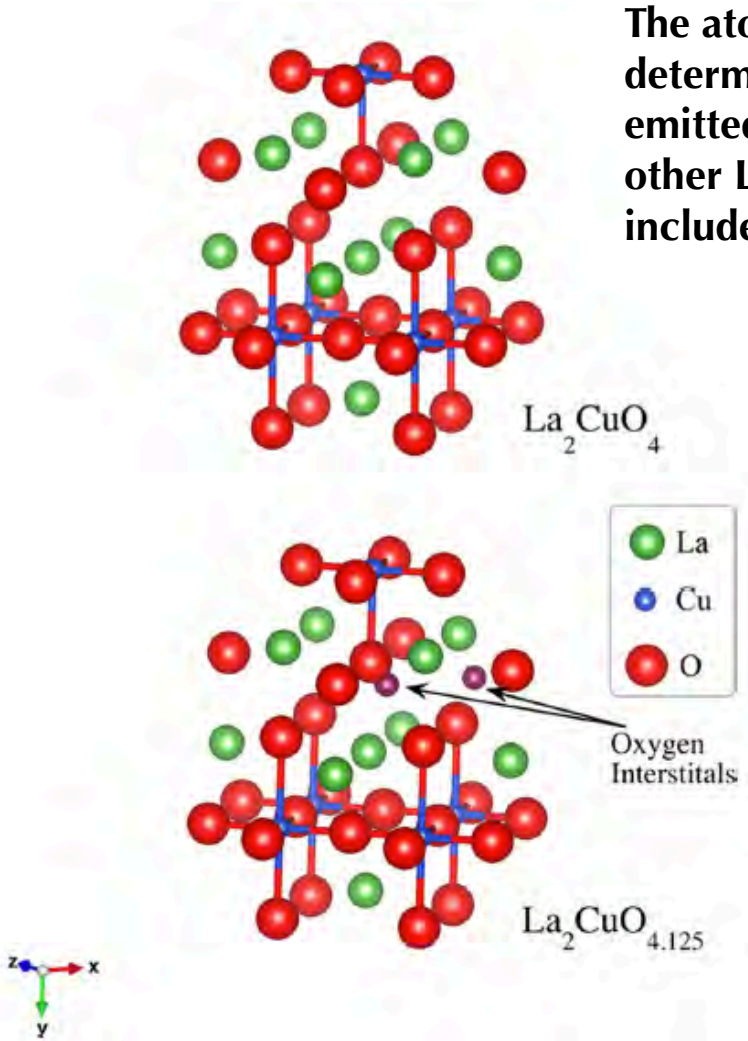

FMS La L_3 XANES calculation for the La_2CuO_4 (brown) and the $La_2CuO_{4.125}$ (black). In the bottom the difference between the two spectra. As shown in the lower panel, Oi induce an increase of the peak due to the first and strongest MSR.

The superimposition of two XANES spectra in the ORPs (La_2CuO_{4+y} with y~0.125 Oi) and in the OPP (La_2CuO_4 without Oi with y~0) shows an increase by 0.4 in units of the La L_3-edge atomic absorption jump and a shift of the white-line in correspondence of the ORP.

FMS theory

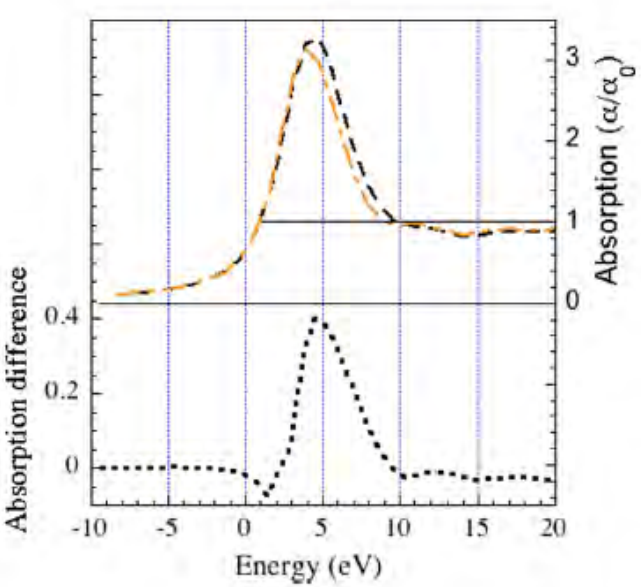

Frascati, October 3, 2017

Istituto Nazionale di Fisica Nucleare

Color maps of the position dependent intensity of the MSR in the XANES spectra of the $La_2CuO_{4.06}$ crystal. Maps are 36x18 pixels (4 µm pixel size). The exposition time was 10 s/step. In (c) are compared the probability density function PDF(x) of the MSR of the ORP and OPP regions.

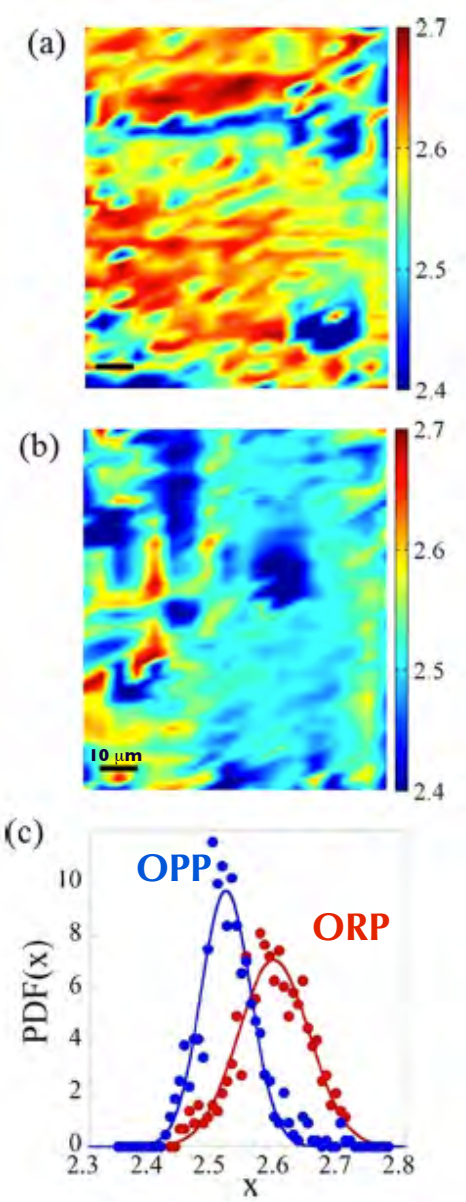

We reconstructed the intensity of the main MSR peak in the XANES spectra using a spot of 4 µm. The spatial distribution of ORPs and OPPs is revealed looking at the MSR peak and comparing the images where different spatial distributions of ORP occur.

The statistical analysis, i.e., the distribution curves of the two regions are shown in panel (c). The x axis is the intensity of the MSR, which ranges from 2.4 to 2.7 in units of the absorption jump. The Gaussian distribution of the map (a) peaked at 2.6 while the map (b) at 2.5 [see panel (c)]. The width of the oxygen poor distribution (OPP) ranges from 2.45 to 2.55, while for the oxygen rich region (ORP) it ranges from 2.52 to 2.65, i.e., we have different distributions in different locations.

The variation of the MSR intensity is smaller respect to the calculation. Actually, as showed by scanning µ-XRD experiments, OPP regions are <4 µm and with our micro-beam it was impossible to probe regions free from ORPs.

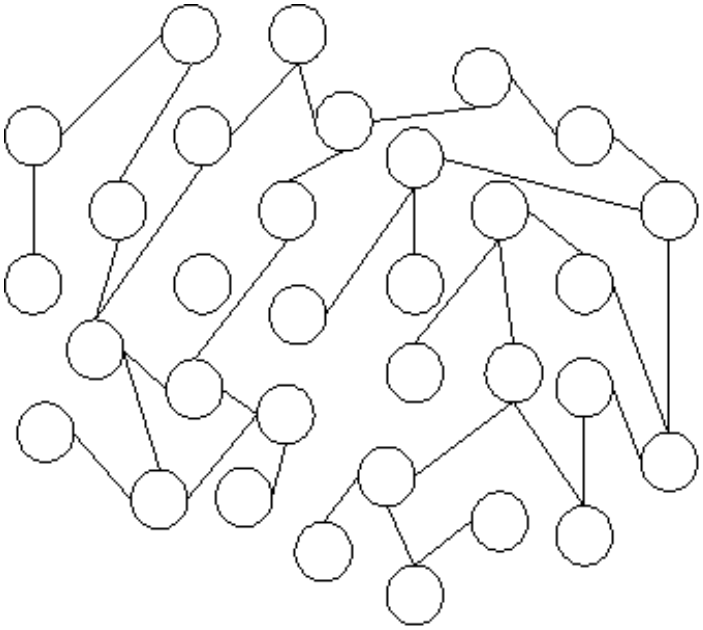

(a) Random network

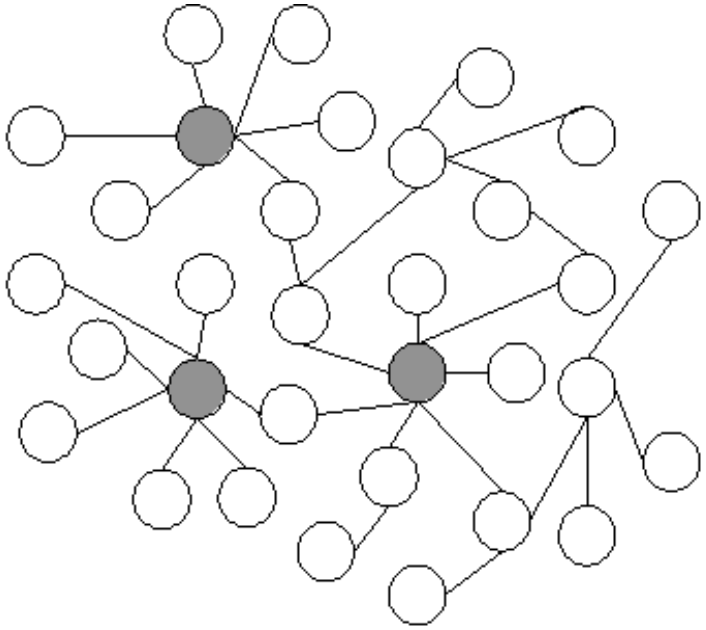

(b) Scale-free network

Frascati, October 3, 2017

Conclusions

- RF applications are limited by operational conditions & materials properties, e.g., yield stress, Young's modulus, etc.;

- TM oxides show many exotic properties and tunable (percolative) conductivity mechanisms;

- Mo oxides intercalated by electron-donating cations may become good conductors, and even metallic. These mixed type conductors show both ionic and electronic conductivity;

- The advantages of cryogenic operation of metallic RF cavities at high field arise from the hardness of the material, the lowered surface dissipation and the concomitant pulsed heating;

- Spectroscopy, diffraction and hyperspectral-imaging techniques are necessary to visualise the nature of metals, alloys and multi-scale systems such as metals, alloys and TM oxides;

- These researches can be extremely useful not only to identify coatings and technology suitable to increase performances of RF cavities working at high frequencies (X-band, W-band, …), but to many other applications where conductivity, field emission, dark current and other properties of technological interest have to be characterised and possibly tuned/optimized.

Frascati, October 3, 2017

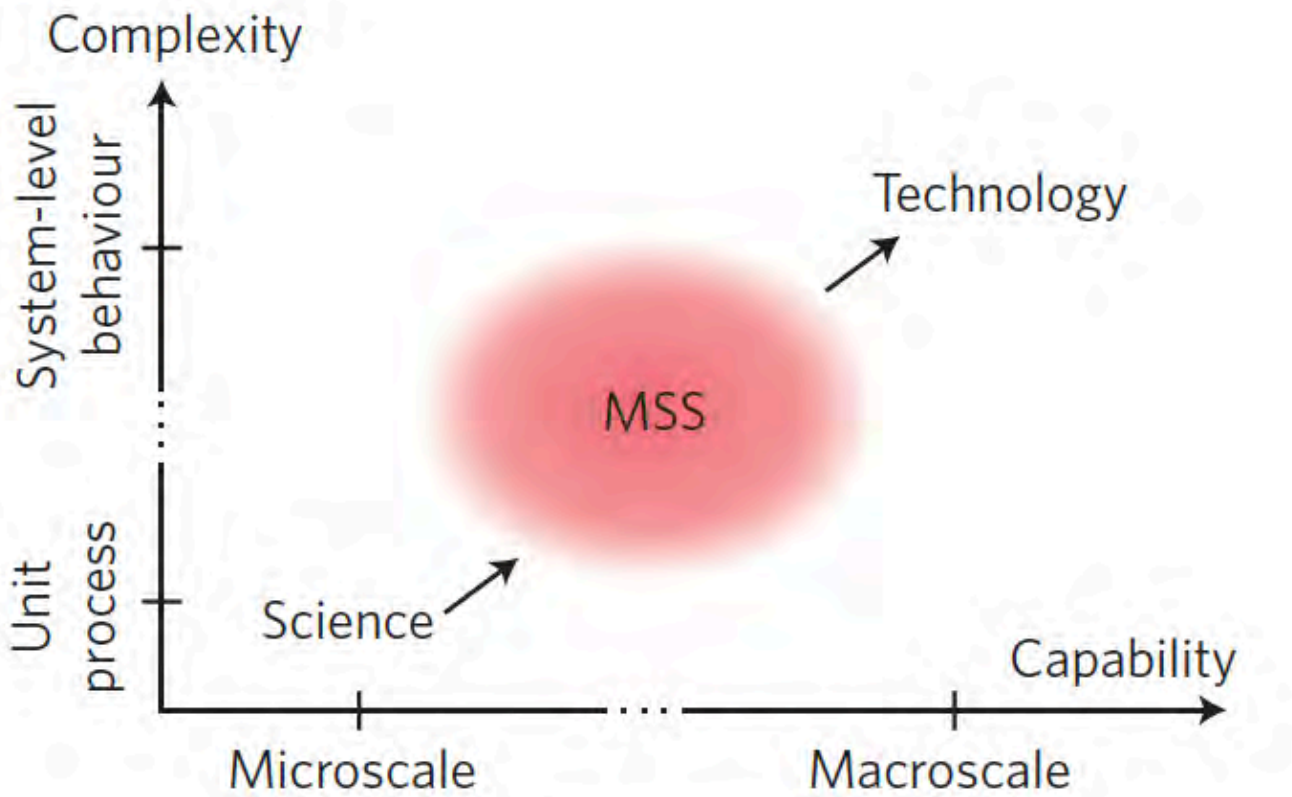

Frascati, October 3, 2017

Acknowledgments

- Antonio Bianconi
- Nicola Poccia
- Stefano Sarti
- Bruno Spataro
- Giannantonio Cibin
- Xu Wei
- Fan Lele
- Chu Wangsheng
- Chong Wen Zhou
- Simone Bini
- Valery Dolgashev
- Salvatore Macis
- Ivan Davoli
- Stefano Lupi
- Giovanni Castorina
- Carmela Bonavolonta'
- .....

marcelli@lnf.infn.it